Testing general relativity with the BepiColombo radio science experiment

Andrea Milani*
Dipartimento di Matematica, Università di Pisa, Via Buonarroti 2, I-56127 Pisa, Italy

David Vokrouhlický†
Institute of Astronomy, Charles University, V Holešovičkách 2, CZ-18000 Prague 8, Czech Republic

Daniela Villani
Hyperborea SCRL, Polo Tecnologico, Via Giuntini 13, 56023 Navacchio, Pisa, Italy

Claudio Bonanno
Dipartimento di Matematica, Università di Pisa, Pisa, Italy

Alessandro Rossi
ISTI-CNR, Area di Ricerca del CNR, Via Moruzzi 1, 56100, Pisa, Italy
(Received 27 September 2001; published 31 October 2002)

The ESA mission BepiColombo will explore the planet Mercury with equipment allowing an extremely accurate tracking. While determining its orbit around Mercury, it will be possible to indirectly observe the motion of its center of mass, with an accuracy several orders of magnitude better than what is possible by radar ranging to the planet's surface. This is an opportunity to conduct a relativity experiment which will be a modern version of the traditional tests of general relativity, based upon Mercury's perihelion advance and the relativistic light propagation near the Sun. We define the mathematical methods to be used to extract from the data of the BepiColombo mission, as presently designed, the best constraints on the main post-Newtonian parameters, especially β, γ and the Nordtvedt parameter η, but also the dynamic oblateness of the Sun $J_{2\odot}$ and the preferred frame parameters α_1, α_2. We have performed a full cycle simulation of the BepiColombo radio science experiments, including this relativity experiment, with the purpose of assessing in a realistic (as opposed to formal) way the accuracy achievable on each parameter of interest. For γ the best constraint can be obtained by means of a dedicated superior conjunction experiment, with a realistic accuracy $\simeq 2\times 10^{-6}$. For β the main problem is the very strong correlation with $J_{2\odot}$; if the Nordtvedt relationship $\eta = 4\beta - \gamma - 3$ is used, as it is legitimate in the metric theories of gravitation, a realistic accuracy of $\simeq 2\times 10^{-6}$ for β and $\simeq 2\times 10^{-9}$ for $J_{2\odot}$ can be achieved, while η itself is constrained within $\simeq 10^{-5}$. If the preferred frame parameters α_1, α_2 are included in the analysis, they can be constrained within $\simeq 8\times 10^{-6}$ and $\simeq 10^{-6}$, respectively, at the price of some degradation in β, $J_{2\odot}$ and η. It is also possible to test the change with time of the gravitational constant G, but the results are severely limited because of the problems of absolute calibration of the ranging transponder, to the point that the improvement as compared with other techniques (such as lunar laser ranging) is not so important.

DOI: 10.1103/PhysRevD.66.082001 PACS number(s): 04.80.Cc, 95.30.Sf, 95.55.Pe, 96.30.Dz

I. INTRODUCTION AND MOTIVATION

A. Historical perspective

Among all bodies in the solar system, Mercury is the best placed to probe the theory of gravitation since it feels more than any other planet the gravity field of the Sun and moves with the highest velocity. Only a few near-Earth asteroids reside on temporarily stable orbits with perihelia closer to the Sun, but their larger semimajor axes decrease the magnitude of the relativistic orbital effects. Moreover, their smaller size results in significant nongravitational forces, with a typically low model accuracy, which perturb their orbit (e.g. [1,2]).

The fascinating story of Mercury's contribution to the tests of the theory of gravitation starts with the Vulcanoid hypothesis by Le Verrier (see, e.g., [3]). Even today, every misfit of the orbital data of cosmic bodies can be approached from two radically different standpoints: (i) either assume the validity of the gravitation theory and seek for the ''missing mass,'' or (ii) put in question the gravitation theory (for the sake of simplicity we neglect in this discussion the role of nongravitational effects). Le Verrier leaned toward the first approach mentioned above. To explain the excess in Mercury's perihelion drift, he postulated the existence of an intramercurian planet named Vulcan. Soon he realized that, if anything, ''Vulcan'' should be a belt of many small bodies rather than a single object. Interestingly, this subject is still alive today (e.g. [4–6]) but the total mass of the Vulcanoid belt, as it is hypothesized now, must be many orders of magnitude smaller than required to cause any observable effects on Mercury's orbit.

At the end of the 19th century, after several decades of unsuccessful search for Vulcanoids and with Newcomb's

*Email address: milani@dm.unipi.it
†Email address: vokrouhl@mbox.cesnet.cz

more complete and precise computation of Mercury's perihelion drift, the problem had a brilliant solution through adopting the second approach: a radical change of the gravitation theory. Although Mercury's perihelion drift was not the primary topic for Einstein to complete his general relativity (GR) theory, he was apparently very excited to realize the new theory explains Newcomb's result (Einstein obtained this result on Nov 18, 1915; see [7]). A little later, in August and September 1916, de Sitter [8] computed precisely enough of this relativistic drift within a fully relativistic formulation of planetary motion and concluded that there was an excellent agreement with the observations.

After the pioneering period, this test of general relativity went into what has been called a ''hibernation period'' [9] because the technologies for more accurate measurements of the orbit of Mercury were not available. Starting in 1959, the new technology of interplanetary radar allowed the measurement of the Earth-Mercury distance with accuracies of a few km. Taking into account that the general relativistic effects displace Mercury with respect to the Newtonian orbit by several tens of km per year, just a few years of data allow to constrain the values of the post-Newtonian (PN) parameters at the level of 1% or better. By accumulating many years of data an estimate of the combination $2\gamma-\beta$ consistent with GR within 0.003 was obtained [10]. Although the radar technology and the knowledge of the plasma effects on radio waves propagation have improved considerably, still today the accuracy of the observations of the orbit of Mercury is limited by the uncertainty of the topographic height of the radar bounce point.

Moreover, the first viewpoint was revived. Dicke [11] introduced another form of ''missing mass'' by postulating that the dynamical oblateness of the Sun, $J_{2\odot}$, could be larger than expected from a rigid rotation of the solar interior, and could contribute to Mercury's perihelion precession and mask deviations of the values of the PN parameters β and γ from their GR value 1. The spectrum of motivations ranged from better accommodation of Mach's principle within the gravitation theory [12] to suggestions that the solar interior might be rotating significantly faster than the surface (perhaps due to the drain of the angular momentum of the solar envelope to the planetary nebula). Although these expectations were not later fulfilled, Dicke was right in prompting a serious investigation of the $J_{2\odot}$ contribution to the observed effects [13]. This is especially true if we are aiming to reach the 10^{-4} or better level in determination of the PN parameters β and γ, since it is easy to see that $J_{2\odot}$ must contribute to Mercury's perihelion motion at this level. Unfortunately the orbit of Mercury is not inclined enough with respect to the solar equator (only 3.3°) to allow for a separation of the β and the $J_{2\odot}$ effects (if the only orbit used is the one of Mercury). Precise independent measurements of the solar quadrupole coefficient are not available: note that the presently available disk-oblateness data [14,15] and the SOHO-GONG measurement of the splitting of the solar normal modes [16] still yield somewhat controversial results. Thus the value of β is currently better measured from lunar laser ranging [17] than from radar ranging to Mercury.

The PN parameter γ appears in the perihelion precession of Mercury but also has other effects, such as the light deflection which can be measured by very high accuracy astrometry. Thus, after the pioneering phase of the measurements of light deflection during a total eclipse, the hibernation period for the experiments on γ ended when the very long baseline interferometry (VLBI) technique became available [10,18]. Moreover, γ appears in the light propagation apparent delay, which can be measured by tracking a spacecraft passing behind the Sun (even if it is not close to the Sun). Experiments based on this principle are under way now [19]. Thus the new generation of Mercury based experiments being designed now need to compete, as far as γ is concerned, also with these independent determinations.

In the context of our work, the Eddington parameters β and γ are regarded as purely phenomenological factors that are to be determined or constrained from the observations. We note, however, that these parameters have a deeper theoretical significance since they are directly linked to the fundamental constants by which the assumed additional scalar fields mediating gravity are coupled to the metric field (see, e.g., [20]). Since the tensor-scalar theories represent the most viable extension of the Einsteinian gravitation theory, their observational verification is very important. We shall thus pay special attention, and devote particular effort, to which level of accuracy our experiment can constrain β and γ.

Nevertheless, there are other parameters which can be determined or constrained together with these two and are by themselves valuable scientific goals. The most important is the Nordtvedt parameter η describing violations of the strong equivalence principle (SEP). Since the late 1960s [21] it was understood that the coupling of gravitation with the self-gravitational energy of a large body could violate the equivalence principle and lead to observable effects in the orbits of the planets and of the Moon. This form of violation is different from the composition dependence of the gravitational constant, which has been the subject of intense experimental efforts in the last decades [22], but as a matter of principle it has to be constrained experimentally.

B. The BepiColombo opportunity

Although there are theoretical arguments [23,24] for the necessity to obtain constraints on β, γ and η well beyond the 10^{-4} level, the state of the art in gravitation theory is such that there is no compelling prediction of the level of accuracy at which a violation of GR would be detected. It has been clear for a long time that a space mission to Mercury, with either a surface long-lasting transponder or an orbiter, could achieve a very significant improvement in the determination of the PN parameters [25–27]. However, to justify such a complex (and expensive) mission uniquely for a relativity experiment, not being able to claim that some violation of GR would be discovered, proved to be difficult.

According to [9], the best way to proceed in the present period with the verification of GR in weak field conditions is to adopt ''an opportunistic approach,'' in which new tests result from available technologies exploited in new ways. Analogously, already planned space missions need to be in-

vestigated to detect opportunities for relativistic experiments, by exploiting as much as possible existing instruments, available spacecraft capabilities and already established mission plans.

The opportunity arose during the European Space Agency (ESA) study for a Mercury Orbiter mission. Two members of the Mercury Orbiter study team, L. Iess and one of the authors (A.M.), proposed a comprehensive radio science experiment which would coordinate a *gravimetry experiment*, a *rotation experiment* and a *relativity experiment*, by processing in a complex way the same data, namely, ultra-accurate range and range rate tracking (based on a higher frequency communication system [29]), the readings from an on-board accelerometer [28], and the images from the most accurate cameras (pointing at both ground features and stars). This experiment was included in the baseline design of the mission, which in the meantime had been renamed *BepiColombo* [30] and is now a fully approved (and funded) ESA mission. To appreciate how good is the ''opportunity'' provided by the BepiColombo mission to Mercury, we need to consider the following features of this mission.

First, the orbit around Mercury of the main spacecraft of the ESA BepiColombo mission, with altitude between 400 and 1500 km [30]. Previous studies assumed much more elliptic orbits. Since the ESA project includes a separated orbiter for the investigation of the Mercury's magnetosphere (requiring a highly elliptic orbit), the main orbiter may reside on a much less eccentric orbit. This is favorable for surface observations but also in the solution for the gravity field and for the center of mass determination for Mercury [31]. The nominal mission plan includes one full year of operations in orbit around Mercury; this paper assumes this nominal duration, although there is always hope for an extension of the mission if the spacecraft main subsystems are found to be robust enough.

Second, the range and range rate measurements will be performed by using a full 5-way link [29] to the main orbiter (the magnetospheric orbiter is not involved in this experiment). By exploiting the frequency dependence of the refraction index, the differences between the delay and Doppler measurements done in the different channels (in the Ka band, in the X band and in mixed mode with both) provide information on the plasma content along the path followed by the radio waves between Earth and the spacecraft orbiting around Mercury. In this way most of the measurement errors introduced, in a single channel, by the plasma can be removed. The expected performances correspond to an improvement of about two orders of magnitude with respect to what was possible with the previous technology, and are briefly discussed in Sec. IV A. Third, we have the on-board accelerometer. Around Mercury the illumination, mostly in visible light from the Sun and mostly in the infrared from Mercury, is fierce (for each of the two sources one order of magnitude larger than the solar flux at the Earth's distance). This results in radiation pressure, which is very difficult to model also because the spacecraft reflects (in the visible) and reradiates (in the infrared) in a very complex way. Thus the propagation of the orbit of an artificial satellite around Mercury is affected by large errors, unless the nongravitational accelerations are measured by an on-board three axis accelerometer. In this case the readings of the accelerometer are just added to the equations of motion containing the gravitational terms only, and the orbit propagation error is controlled by the accelerometer measurement error (see Sec. IV A), which is typically two orders of magnitude less than the perturbations. This allows an orbit determination with unprecedented accuracy (for an interplanetary probe).

C. Purpose of this work

Given the need for tighter verification of GR or detection of its smaller violations, if any, and given the opportunity represented by the BepiColombo mission to Mercury, our purpose is to establish which of the PN parameters can be determined, and with which accuracy, given the current mission design and instrument performance assumptions.

Although the choice of the PN parameters and solar system model constants to be determined is discussed in full in Secs. II and IV, we need to anticipate that our choice of the target PN parameters is somewhat different from the one in previous studies. In comparison with the study of Ashby, Bender and Wahr [27], we neglect some parameters we consider of less importance; however, we include the planetary test of the strong equivalence principle (due to the polarization of Mercury's and Earth's orbits in the gravity field of Jupiter; see [32]). In fact, the solution for the related Nordtvedt parameter η may be employed to remove the correlation between the solution of β and the $J_{2\odot}$, which used to be the weak point of the Mercury-based tests of GR.

The main achievement of our work consists of performing a full cycle of numerical simulation of the radio-science experiment of BepiColombo, out of which the determination of the relativistic parameters is only a part. Since the solution for the gravitational field of Mercury and other parameters may in principle produce systematic effects in the observables used to determine the relativistic parameters, it is of fundamental importance to adopt this global approach. In this way, ''internal'' systematic effects may result from the correlated solution of different parameters, but we also test the influence of the ''external'' systematic effects due to possibly biased observations. These latter include both effects on ranging measurements, such as the degradation of the on-board transponder, but also correlated noise in the on-board accelerometer readings. Details of our strategy has been outlined in Ref. [33] and will be recalled only to a minimum extent related to the solution for the relativistic parameters, the main focus in this paper.

The paper is organized as follows: in Sec. II we give a brief overview of our approach and the necessary mathematical formulas to evaluate the effects of the different ways of violations of GR; some results required for the evaluation of the effects of violating the strong equivalence principle are relegated to the Appendix. In Sec. III we present in two separate steps the methods used to fit the data to solve for the mercurycentric orbit of the satellite and for the orbit of the planets. In Sec. IV we discuss the simulations and their results, and conclude in Secs. V and VI with indications for the work to be done between now and the time of the experiment

and with an assessment of the quality and value of these results.

II. MATHEMATICAL FORMULATION

Within the metric theories of gravitation, each violation of the principles of GR is reflected in a corresponding modification of the space-time metric and thus affects all sectors of the observation model: (i) the connection between local and global coordinate systems, (ii) the equations of motion, and (iii) the propagation of the electromagnetic signal.

The coordinate transformation effects [34,35]—item (i) above—are too small to probe the PN parameters. For instance, the transformation between the barycentric and geocentric coordinate systems alters the position of an Earth station by about 6 cm in general relativity. Though we take this effect into account, we do not consider its dependence on the PN parameters (γ in particular). Moreover, we shall not introduce in this work a truly relativistic local reference frame (and time scale) of Mercury but rather formally express the spacecraft solar system barycentric position with respect to Mercury.

The relativity test then consists of investigating the PN parameter dependence of the equations of motion and the propagation effects [items (ii) and (iii) above]. The role of the equations of motion in our approach deserves a brief discussion. As is usual, the satellite motion is best referred to the planet it is orbiting around. The solar system state vector of the spacecraft (that enters in definition of the observables, i.e. the delay and Doppler shift measurements) is then composed of the local motion of the satellite and the motion of Mercury's center of mass in the solar system. Both these components are affected by the relativistic (i.e. $\propto 1/c^2$) perturbations in their own way. It can, however, be easily seen that the satellite local dynamics, i.e. the motion around Mercury's center of mass, does not have the capability of probing these phenomena. Indeed, like in the lunar case, the largest effect is the geodetic precession due to the solar gravity field (the perihermian drift due to Mercury's relativistic monopole gravity is significantly smaller). The geodetic precession can be represented as a constant rotation of the spacecraft orbit with respect to distant stars, resulting in a displacement of about 30 cm over one month. This value is far too small to be detected. The method we use to solve for the mercurycentric motion, discussed in Sec. III A, essentially gives up any attempt to define a long term reference system based upon the satellite orbit. In fact, the local dynamics of the satellite around Mercury is modeled with sufficient accuracy by purely Newtonian equations of motion.

Thus it is only the Mercury's center of mass heliocentric motion that is capable of determining the PN parameters. The output of the mercurycentric orbit determination, used as input for the orbit determination of the planet, contains only a set of ''synthetic observations'' of the Earth-Mercury range and range rate, one for each of the arcs in which we split the satellite orbit (see Sec. III B). This two-dimensional observation of Mercury's heliocentric motion is at a level of accuracy superior to the ground-based radar measurements, both because of the higher frequencies and plasma compensation scheme and because the ''equivalent bounce point'' is the center of mass of the planet, without loss of accuracy due to topographic model problems. These observations may be confronted with a theoretical model depending on the PN parameters. Obviously, the light propagation relativistic effects in both range and range rate should be taken into account. This happens mainly when Mercury gets in superior conjunction with the Sun as seen from Earth.

In the next two subsections the relevant orbital effects and the light-propagation relativistic effects are summarized at the level needed for our study.

A. The orbital effects

The most compact way to describe the orbital effects related to the PN parameters is to express them through additional terms in the Lagrangian describing the planetary dynamics (which follow in a straightforward way from the corresponding terms in metric). Let us assume that the motion of the planets, as given by the Jet Propulsion Laboratory (JPL) ephemerides, is described by the Lagrangian L_{GR}, used here as a zero order approximation. The subscript GR indicates that all necessary Newtonian and general relativistic effects have been considered [36]. Since the BepiColombo data are of superior quality to those used in construction of the JPL ephemerides, we assume that their description needs an extended dynamical framework that can be given by the Lagrangian

$$L(\bar{\beta},\bar{\gamma},\bar{\delta},\alpha_1,\alpha_2,\dot{G}/G,\ldots) = L_{GR}+\{L_{\bar{\beta}}+L_{\bar{\gamma}}+L_{\bar{\delta}}+L_{\alpha_1}+L_{\alpha_2}+L_{\dot{G}/G}+\ldots\}, \tag{1}$$

with the new terms in the curly brackets. These latter terms are individually linked to some of the parameters to be determined, such as $\bar{\gamma}=\gamma-1$ and $\bar{\beta}=\beta-1$. Hereafter we briefly overview their nature, but refer to earlier studies for a more detailed analysis. The classical textbook [13] is a general reference here.

The velocity-dependent modification of the two-body interaction is parametrized by the Eddington parameter $\bar{\gamma}=\gamma-1$:

$$L_{\bar{\gamma}}=\frac{1}{2c^2}\bar{\gamma}\sum_{A\neq B}\frac{GM_AM_B}{r_{AB}}\mathbf{v}_{AB}^2, \tag{2}$$

while the modification of the non-linear three-body general relativistic interaction depends upon the Eddington parameter $\bar{\beta}=\beta-1$ through

$$L_{\bar{\beta}}=-\frac{1}{c^2}\bar{\beta}\sum_{A\neq B,C}\frac{G^2M_AM_BM_C}{r_{AB}r_{AC}}. \tag{3}$$

Here $\mathbf{v}_{AB}$ denotes the mutual (barycentric) velocity of the body A with respect to the body B, r_{AB} their mutual (barycentric) distance and c the speed of light. Since we are dealing with gravitational interaction, the definition of the constants G and M_A deserves a special attention: G denotes the

coupling constant for the composition-independent part of the gravitational interaction and M_A denotes the inertial mass of the body A.

The second type of the orbital effects to be included in our study are caused by a possible violation of the equivalence principle. They can be described by an additional Lagrangian term

$$L_{\bar{\delta}} = \frac{1}{2} \sum_{A \neq B} (\bar{\delta}_A + \bar{\delta}_B) \frac{G M_A M_B}{r_{AB}}, \tag{4}$$

with

$$\bar{\delta}_A = \hat{\delta}_A + \eta \frac{E_A^{\rm grav}}{M_A c^2}, \tag{5}$$

and represent the combined effect of the composition-dependent gravitational couplings [$\hat{\delta}_A \neq 0$; violation of the ''weak equivalence principle'' (WEP)] and of the Dicke-Nordtvedt contribution due to the coupling with the gravitational self-energy [$\eta \neq 0$; violation of the ''strong equivalence principle'' (SEP)]. Within the frame of the metric theories of gravitation, the parameter η is related to the other PN parameters through the relation $\eta = 4\bar{\beta} - \bar{\gamma} - \alpha_1 - \frac{2}{3}\alpha_2$ [13,37,38]. It can be easily checked that the BepiColombo data do not have the capability to bring new results regarding WEP, since the laboratory and lunar laser ranging experiments constrained WEP with a higher precision [13,17]. On the other hand, exploiting the large value of the solar gravitational self-energy [$(E_\odot^{\rm grav}/M_\odot c^2) \simeq -3.52 \times 10^{-6}$], our experiment may result in better constraining the SEP through a tighter limit on the parameter η.

The effect of η in the planetary equations of motion is twofold: (i) it contributes to a redefinition of the solar and planetary masses and (ii) it produces a polarization of the Mercury and Earth orbit around the Sun in the gravitational field of other planets (mainly Jupiter). However, the bulk of the first effect can be interpreted as an unobservable redefinition of the gravitational constant in the solar system, namely: $G \to G_\star = G[1 + \eta (E_\odot^{\rm grav}/M_\odot c^2)]$. In what follows we assume such a recalibration of G and we shall focus on orbit perturbations due to the polarization phenomena (ii). Since this is a somewhat delicate issue, we devote the Appendix to a closer description of the related perturbation of Mercury's orbit (see also the discussion in [26,32]).

As gravity is a long-range force, one might *a priori* expect the universe's global matter distribution to select a preferred rest frame for local gravitational physics. As shown in [13,39,40], the preferred frame effects in the first post-Newtonian limit are phenomenologically describable by as many as six parameters, but only two of these, α_1 and α_2, can be different from zero without violating some fundamental theoretical constraints [41]. These parameters are associated with the following terms in the Lagrangian describing the gravitational dynamics of N-body systems:

$$L_{\alpha_1} = -\frac{\alpha_1}{4} \sum_{A \neq B} \frac{G M_A M_B}{r_{AB} c^2} (\mathbf{v}_A^0 \cdot \mathbf{v}_B^0), \tag{6a}$$

$$L_{\alpha_2} = \frac{\alpha_2}{4} \sum_{A \neq B} \frac{G M_A M_B}{r_{AB} c^2} [(\mathbf{v}_A^0 \cdot \mathbf{v}_B^0) - (\mathbf{n}_{AB} \cdot \mathbf{v}_A^0)(\mathbf{n}_{AB} \cdot \mathbf{v}_B^0)]. \tag{6b}$$

Here, $\mathbf{v}_A^0$ represents the velocity of body A with respect to the gravitationally preferred frame. Many (though not all) of the observable effects linked to α_1 and α_2 depend on the choice of the gravitationally preferred frame. We shall follow the standard assumption [13] that the latter frame, being of cosmological origin, can be (at least approximately) identified with the rest frame of the cosmic microwave background. This means that the center of mass of the solar system has the velocity $\mathbf{w}$ with respect to the preferred frame of rest, with $|\mathbf{w}| \simeq 370 \pm 10$ km/s in the direction $(\alpha, \delta) = (168°, -7°)$ [42–44]. The cosmic velocity of a body A then reads $\mathbf{v}_A^0 = \mathbf{w} + \mathbf{v}_A$, where $\mathbf{v}_A$ is the velocity of the body with respect to the center of mass of the system. Notice that $\mathbf{w}$ is larger than $\mathbf{v}_A$, but the Mercury's perihelion velocity (≈ 58 km/s) is not much smaller (thus the Mercury test of the preferred-frame effects is different from the corresponding tests using the dynamics of satellites of the Earth, e.g. [45]). In what follows, we have neglected a term quadratic in the cosmic velocity $\mathbf{w}$ in Eqs. (6), since it is equivalent to a constant redefinition of the gravitational parameter $G \to G[1 - (\alpha_1 - \alpha_2) w^2/4c^2]$ in the solar system and thus does not lead to observable effects.

Many alternative theories of gravitation also allow for the time dependence of the gravitational coupling constant (e.g., because of the cosmological evolution of some coupled scalar fields). Since the characteristic time scale is comparable to the inverse of the Hubble constant, the solar system experiments could probe just the rate by which G changes (e.g. [13]). The corresponding dynamical effect, parametrized by $d(\ln G)/dt$, is expressed by the Lagrangian

$$L_{\dot{G}/G} = t \frac{d(\ln G)}{dt} \sum_{A \neq B} \frac{G M_A M_B}{r_{AB}}, \tag{7}$$

where t is time measured from some conventional origin. It is well known that this perturbation produces mainly a quadratic change in the planetary longitude in its orbit (e.g. [46]).

Together with testing the PN parameters we must consider other ''Newtonian'' effects that may cause their mismodeling. These effects belong to two classes: (i) Newtonian parameters that have been taken into account in the JPL ephemerides, but their uncertainty produces orbital effects comparable to or larger than the expected perturbation due to the tested relativistic effects, and (ii) effects not modeled by the JPL ephemerides (e.g., the gravitational perturbations of some asteroids). In our solution we shall consider (i), but the effects of (ii) will not be modeled directly; see the discussion in Sec. VI.

The first class, (i), includes essentially two effects: a small change in the solar mass and a small change $\delta J_{2\odot}$ in its quadrupole coefficient $J_{2\odot}$ (characterizing the solar gravity-field ''oblateness''). As mentioned above, the second term

has been considered for a long time as a primary cause of the uncertainty in Mercury's perihelion modeling, but at the level of precision of the Mercury orbiter data even the first effect has to be taken into account.

Apart from the previously considered set of PN parameters $(\overline{\beta},\overline{\gamma},\eta,\alpha_1,\alpha_2,\dot{G}/G)$, we shall thus extend our model by two more parameters μ and $\delta J_{2\odot}$. The first characterizes a fractional change of the solar mass ($\mu=\Delta M_\odot/M_\odot$) and the second characterizes change of the solar $J_{2\odot}$ coefficient (the JPL DE405 ephemerides use a value of 2×10^{-7}). The corresponding Lagrangians are

$$L_\mu=\mu\sum_{A\neq\odot}\frac{GM_\odot M_A}{r_{A\odot}},$$
$$L_{\delta J_{2\odot}}=-\frac{\delta J_{2\odot}}{2}\sum_{A\neq\odot}\frac{GM_\odot M_A}{r_{A\odot}}\left(\frac{R_\odot}{r_{A\odot}}\right)^2[3(\mathbf{n}_{A\odot}\cdot\mathbf{e}_\odot)^2-1], \tag{8}$$

where $M_\odot$ is the solar mass, $R_\odot$ its radius, $\mathbf{r}_{A\odot}$ is the heliocentric position of the body A, $\mathbf{n}_{A\odot}$ is the corresponding unit vector and $\mathbf{e}_\odot$ is the unit vector along the solar rotation axis. This latter is slightly tilted from the normal to the ecliptic plane as described in [47].

Obviously, our analysis also contains a solution of state vectors of the Earth and Mercury at some epoch, but this requires taking into account suitable constraints, as discussed in Sec. III B.

Given the Lagrangian terms which, in our approach, extend the standard description of the planetary motion, we shall investigate their orbital effects. Let $\mathbf{r}_A$ be the solar system barycentric position of the Ath body. Then the standard model, represented by the JPL ephemerides, yields a solution of

$$\frac{d^2\mathbf{r}_A}{dt^2}=-\sum_{B\neq A}\mathbf{g}_{AB}+\mathbf{p}_A, \tag{9}$$

where $\mathbf{g}_{AB}=GM_B\mathbf{r}_{AB}/r_{AB}^3$, $\mathbf{r}_{AB}=\mathbf{r}_A-\mathbf{r}_B$ and M_B is the mass of body B; $\mathbf{p}_A$ abbreviates a large number of perturbing terms due to higher-degree multipole Newtonian effects, tidal phenomena and GR post-Newtonian effects ($\propto1/c^2$).

In what follows, we shall consider a small variation $\Delta\mathbf{r}_A$ of the JPL-determined planetary positions ($\mathbf{r}_A\to\mathbf{r}_A+\Delta\mathbf{r}_A$). Obviously, we assume that the magnitude of $\Delta\mathbf{r}_A$ remains within the uncertainty tube of the JPL solution and we study how it may be constrained by the very precise measurements of the BepiColombo radio-science experiment. Omitting the quadratic (and higher order) terms, the planetary displacements $\Delta\mathbf{r}_A$ satisfy

$$\frac{d^2\Delta\mathbf{r}_A}{dt^2}=-\sum_{B\neq A}\frac{GM_B}{r_{AB}^3}\Delta\mathbf{r}_{AB}+3\sum_{B\neq A}(\mathbf{r}_{AB}\cdot\Delta\mathbf{r}_{AB})\frac{\mathbf{g}_{AB}}{r_{AB}^2}+\sum_\epsilon\left\{\frac{\partial L_\epsilon}{\partial\mathbf{r}_A}-\frac{d}{dt}\frac{\partial L_\epsilon}{\partial\mathbf{v}_A}\right\}, \tag{10}$$

with the same notation as before, and ϵ stands for any of the parameters introduced above. We shall not give here a straightforward, but lengthy, expression for the terms in large curly brackets at the right-hand side of Eq. (10). We only note that the sensitivity of the planetary ranging data on the Nordtvedt parameter η is discussed explicitly in the Appendix.

Notice that in Eq. (10) we have neglected the ''second order'' effect due to the variation of the planetary state vectors in the smaller terms $\mathbf{p}_A$, but we need to retain the corresponding variations from the dominant terms (i.e. $-\Sigma_B\mathbf{g}_{AB}$). Out of these, the free variations of the Keplerian heliocentric motion are the most important, also because of their frequency spectrum. It contains the anomalistic revolution frequency of the planet (and its multiples for an eccentric orbit like that of Mercury). Whenever these frequencies are close to those of the analyzed perturbations [the terms in large curly brackets in Eq. (10)], a resonant amplification appears. Notably, the preferred frame effects related to the α_1 and α_2 parameters mainly depend on the sidereal mean motion frequency. In theory, the slight difference between Mercury's anomalistic and sidereal frequencies should suitably amplify the corresponding perturbation and also allow decorrelation from other effects. In practice, however, the two frequencies are too close to each other (due to the slow perihelion motion of Mercury). Thus it is not easy to decorrelate them from the other perturbations that mainly act at the anomalistic frequency. These preliminary considerations help in better understanding the results reported in Sec. IV.

B. The light-propagation effects

Simulation and analysis of the radio-science data for the BepiColombo satellite are demanding, mainly because of complicated aberration effects. The classical astronomical methods, even those used for satellite geodesy, do not meet the required accuracy. Note that the light distance to the satellite from the Earth telescope may be up to 11 min, and during this time both planets and the spacecraft move by a significant distance. A rigorous tracing of the radio beam from the telescope, at the instant of transmission, to the satellite, at the instant of retranslation, and back to the Earth antenna, at the instant of reception, is programmed. This procedure bears similarities with that used for radar tracking of the near-Earth asteroids (e.g. [48]), but it is more complicated, since visibility of the satellite might become violated between transmission and the eventual retransmission by the satellite. The time readings at the transmission and reception are assumed in the terrestrial time (equivalent to the coordinated atomic time scale), but these are then referred to the solar system barycentric time scale by usual transformations.

The range-rate measurements with the accuracy indicated in Sec. II A require inclusion of the quadratic Doppler effect. The third-order Doppler effect $\propto(v/c)^3$, on the level of the measurement accuracy, has been also included in our computation. Though these terms are necessary for interpreting the data, they do not probe the gravitation theory.

On the contrary, the accumulated delay effect along the path of the radio beam toward the spacecraft and back to Earth—the Shapiro effect at the PN level of accuracy—is sensible to the value of the PN γ parameter. At the level of

accuracy of ranging to Viking landers ($\simeq 7$ m), only the first order effect was needed and led to a tight constraint of γ [10]. With an accuracy in range at the decimeter level, the second order light-time effect should be accounted for [49] (note that the solar quadrupole influence is negligible in this respect [50]). However, it is still the first order (Shapiro) term that solely has the capability to constrain the γ parameter. Put in terms of an equivalent change of Mercury's distance from the telescope along the light of sight, we have

$$\Delta R = \frac{1+\gamma}{2}\frac{GM_S}{c^2}\ln\left(\frac{r_1+r_2+r_{12}}{r_1+r_2-r_{12}}\right)+(\Delta R)_{GR}, \qquad (11)$$

where $\mathbf{r}_1$ is the heliocentric position vector of the observing station ($r_1=|\mathbf{r}_1|$), $\mathbf{r}_2$ is the heliocentric position vector of the spacecraft ($r_2=|\mathbf{r}_2|$) and $\mathbf{r}_{12}=\mathbf{r}_1-\mathbf{r}_2$ ($r_{12}=|\mathbf{r}_1-\mathbf{r}_2|$). In Eq. (11) we give explicitly only the part depending on γ, while the Einsteinian terms, including the higher-order delay and the aberration terms of the $\propto 1/c^3$ level, are denoted by $(\Delta R)_{GR}$. Note that the α_1 parameter appears in ΔR at the $\propto 1/c^3$ level, but given the current knowledge of this parameter this term can be considered as known to the required accuracy.

Bertotti *et al.* [19,51,52] have also discussed the gravitational Doppler shift corresponding to the effective change in the overall optical distance to the spacecraft. This is the base of the proposed experiment with the Cassini conjunctions, which is being done now [19]. As discussed in Sec. IV A the Doppler measurements at the superior conjunction of BepiColombo cannot give constraint on the γ parameter superior to the orbital solution from one year of observations. Thus the Cassini experiment, with a Doppler measurement accuracy equivalent to the one assumed for BepiColombo, should improve the current knowledge of γ, but not as much as the experiment we are now proposing. The superior conjunction experiment (Sec. III C) thus fundamentally relies on the delay measurements and their analysis through Eq. (11).

Finally, we should comment on the role of the plasma in the solar corona for the time delay. In what follows, we assume a perfect compensation of this effect by using a dual ranging in X and Ka bands [29]. It has been estimated [53] that down to ≈ 3 solar radii the size of the turbulent cells in the coronal environment is typically smaller than the difference of the impact parameters for the X and Ka-band beams: under these conditions the data in the two frequencies may be successfully used to compensate the plasma effects. Thus we have assumed, in the simulation of our superior conjunction experiment, that the data are without degradation until the Mercury-Sun angle, as seen from Earth, is 0.7°, and no data at all below this limit: of course this is a simplification, in reality the data would gradually degrade in accuracy around this boundary.

III. ORBIT DETERMINATION AND PN PARAMETERS SOLUTION

An experiment for the determination of the PN parameters by tracking a Mercury orbiter uses as observables the range and range rate between the satellite and Earth [54] (for a description of the BepiColombo tracking method and geometry see Sec. IV). The variables to be solved include not only the PN parameters, but also the parameters defining the mercurycentric satellite orbit and the parameters defining a solar system model. The latter include the initial conditions for the heliocentric orbits of the planets and parameters, such as masses and PN parameters, appearing in the planetary equations of motion. The orbit of the satellite depends upon its initial conditions and upon the parameters appearing in the mercurycentric equations of motion, such as the mass of Mercury and the harmonic coefficients of the gravity field of the planet. We are not discussing here the nongravitational perturbations, which are important but are handled in the BepiColombo experiment with the special technique already outlined in Sec. I B.

As a matter of principle we could use all the observations, that is range and range rate measurements taken over the entire operational time span of the assumed Mercury orbiter, and solve for all the parameters: the ones of interest for this experiment, the ones which serve other purposes and even the ones which serve no scientific purpose at all but need to be included in the solution because their value is not well enough known *a priori* (e.g., the initial conditions of the satellite). The computational complexity for such a single-step solution is so high that we could run only a limited number of simulations. On the contrary we are interested in testing different assumptions and even in exploring the statistical properties of a large set of simulations, to identify systematic effects as well as random ones. To limit computational complexity and to have a better insight in the physics of the problem we have developed an original method separating the global solution into two separate steps. In the first step the mercurycentric orbit of the satellite is determined, together with the synthetic range and range rate observations of Mercury. In the second step the orbits of Mercury and the Earth are determined, together with the PN parameters.

This section is organized as follows: Sec. III A presents the multiarc method, which is used to determine the satellite orbit taking into account the problems resulting from inaccuracy of the dynamical model. Section III B presents the PN corrector, which solves for the orbits of Earth and Mercury as a single arc, taking into account the complicated geometric properties resulting from symmetries and constraints. Section III C describes the only case in which the two step method does not need to be used (and indeed has not been used in our simulations), the so-called superior conjunction experiment. It solves separately for γ by exploiting a short time span during which the radio waves pass close to the Sun in their path from Earth to the satellite and back.

A. The multiarc method

As a matter of principle, the trajectory of a spacecraft can be considered as a single orbit, depending upon a single set of initial conditions and upon the parameters appearing in the equations of motion. However, the equations of motion depend upon a theoretically infinite (and practically extremely large) set of parameters, out of which only those with larger effects can be determined. To attack this problem it is cus-

tomary, in the orbit determination problems of satellite geodesy, to separate the set of dynamical parameters into two subsets: the ones corresponding to well understood, and explicitly modeled, perturbations and the ones introduced only to absorb the effects which cannot be modeled accurately enough. This technique allows us to reduce the observation residuals, therefore to improve the determination of the parameters of interest, but the values of the additional parameters are not physically significant, at least not directly. To understand the need for such a method, in our case, note that in Ref. [33] we have determined that the systematic, low-frequency components in the accelerometer measurement errors result in about 10 m uncertainty of the satellite position after one day.

Among the methods used to realize this over-parametrization of the problem, the multiarc method decomposes the orbit in arcs, each one with its separate initial conditions. There is no constraint, for the initial conditions of some arc, to coincide with the propagation at the new initial time of the orbit with the initial conditions of the previous arc. This violation of the causal connection between arcs, as if they did not belong to the same physical body, allows for unmodeled perturbations for which the explicitly known equations of motion cannot account. Since the low-frequency noise of the accelerometer may cause orbital error propagating up to $\propto t^2$, short arcs, not longer than a few hours, are needed to meet the requirement of accumulated orbit errors comparable to the accuracy of ranging.

There are different versions of the multiarc method; we are following the formulation of [55]. The basic idea is as follows: the set of observations are subdivided into arcs, belonging to non-overlapping time intervals. The orbit is computed, for arc i, only starting from an initial condition (mercurycentric position $\mathbf{s}_i$ and velocity $\dot{\mathbf{s}}_i$) corresponding to a reference time t_i belonging to the arc time span. Then the observations of arc i do not depend upon the initial conditions of arc j for $i \neq j$. The initial conditions $(\mathbf{s}_i, \dot{\mathbf{s}}_i)$, possibly together with other parameters affecting only the observations of arc i, form the set of *local parameters* ℓ_i. The union of the local parameters for all the arcs forms the vector $\mathcal{L}$ of all the local parameters. All the observations also depend upon a set of *global parameters* $\mathcal{G}$, such as the mass and gravitational harmonic coefficients of the planet; the global parameters are the same for each arc, that is, they are assumed not to depend upon time [56].

A suitable mathematical technique allows us to solve for both $\mathcal{L}$ and $\mathcal{G}$ in such a way that the principle of least squares (for the observation residuals) is satisfied. This can be achieved without inversion of the full normal matrix (which could be too large for numerical stability), and this solution is exact, in particular does not neglect the fact that local and global parameters become correlated. In this way we can check whether it is indeed possible to separate the determination of all parameters in two steps, one to solve the global parameters and one to use separately the local parameters, as determined, like observables for a separate fit: for this procedure to be legitimate, the local-global correlations need to be low [57].

The need to decompose the orbit of a Mercury orbiter into arcs, the way to select the time intervals according to the natural time structure of the set of observations (depending upon the visibility conditions for the spacecraft from a ground station) and the problem of selecting the arc length in a way appropriate to absorb the unmodeled non-gravitational perturbations are discussed in [33]. Here we would like to discuss only which parameters are to be considered global and which local.

The observations of arc i depend upon the position and velocity of Mercury's center of mass at the observation time. Let $\Delta\mathbf{M}(t)$ be the difference between the actual position of Mercury and the reference orbit, which we assume to result from an exact GR orbit propagation for all planets [36]; let $\Delta\dot{\mathbf{M}}(t)$ be the corresponding difference in velocity. The changes with time of these quantities are slow (with respect to the duration of an arc, i.e., few hours), thus we can use the values $\Delta\mathbf{M}_i = \Delta\mathbf{M}(t_i), \Delta\dot{\mathbf{M}}_i = \Delta\dot{\mathbf{M}}(t_i)$ for all the observations of arc i. In principle the values $\Delta\mathbf{M}_i$ are causally connected, namely there is a single arc orbit of Mercury. However, to allow for the decoupling of the orbit determination of Mercury from the one of the satellite, we consider them to be independent. Thus the list of local parameters could include 12 parameters $\ell_i = (\mathbf{s}_i, \dot{\mathbf{s}}_i, \Delta\mathbf{M}_i, \Delta\dot{\mathbf{M}}_i)$. As we will see in the next section, this number of parameters needs to be reduced to account for symmetries. However, some parameters concerning the orbit of Mercury can be determined in the first step multiarc solution and fed as observations to the second step. To ignore, in the second-step fit, the initial conditions of the satellite requires that the correlations among them and the corrections to the orbit of Mercury be small (if this was not the case, a corrected orbit of Mercury could be used in a second iteration of the first step). The global parameters $\mathcal{G}$, in the first step fit, include the goals of the *gravimetry experiment*, whose results are in this way decoupled from the results of the *relativity experiment*, which results from the second-step fit. The results of the gravimetry experiment, as well as many other details we do not need to repeat here, are discussed in [33].

B. The PN corrector

A common problem in orbit determination is that the *normal matrix*, the coefficient matrix of the normal system to be solved to obtain the least squares solution, is badly conditioned [58]. As a result, there are directions (in the space of parameters being determined) along which the uncertainty of the solution is large, even if the fit is good (i.e., the observation residuals are small). Obviously this phenomenon needs to be controlled to avoid results much poorer than expected.

It is known [59] that whenever there is an exact symmetry, that is a Lie group of transformations of the parameter space such that all the observations, both in range and in range rate, are left invariant, then the normal matrix is degenerate, with k null eigenvalues if the dimension of the group is k [60]: in this case the problem is said to have *rank deficiency of order k*. When the symmetry is broken but still holds approximately, that is the change in the observations contains a small parameter ϵ, then the normal matrix has the

same number k of eigenvalues of the order of ϵ^2: in this case the problem is said to have an *approximate rank deficiency of order k*.

The normal matrix for the set of 12 parameters $\mathbf{s}_i, \dot{\mathbf{s}}_i, \Delta\mathbf{M}_i, \Delta\dot{\mathbf{M}}_i$ has an approximate rank deficiency of order 5. The small parameters are the small angle $\Delta\theta$ by which the Earth-Mercury vector is changing over the time span of one arc, the ratio s/R between the satellite-Mercury and the Earth-Mercury distances and the relative size ϵ of the perturbation from the Sun with respect to the gravitation of the planet (e.g., ϵ can be the Roy-Walker parameter [61,62]). The approximate symmetry group contains the full three-dimensional group of rotations (centered on the Earth) applied simultaneously to both Mercury and the spacecraft. This would be an exact symmetry, that is both the range and range rate to the spacecraft would be invariant, if we could neglect the motion of Mercury over the time span of one arc. Additionally there are the approximate symmetries obtained by changing the components of $\Delta\dot{\mathbf{M}}_i$ orthogonal to the Earth-Mercury vector $\mathbf{R}_i = \mathbf{R}(t_i)$. Such a change in the velocity of Mercury changes the range rate only, and by an amount containing the small parameter (s/R).

This degeneracy can be cured by a combination of two changes to the fit. First, the parameters to be solved are limited to 8: $\mathbf{s}_i, \dot{\mathbf{s}}_i, \Delta R_i, \Delta\dot{R}_i$, where $\Delta R_i = \Delta R(t_i)$ is a change in the Earth-Mercury distance $R(t_i)$, at the reference time of arc i; similarly for $\Delta\dot{R}_i = \Delta\dot{R}(t_i)$. Second, after this reduction there is still an approximate rank deficiency of order 1, with as a symmetry group the rotations around $\mathbf{R}_i$. It can be shown, with the same technique used in [59], Section 3, that there are no other symmetries (apart from the particular cases in which the satellite orbital plane either contains or is orthogonal to the Earth-Mercury direction). As discussed in the same paper, Section 6, there are three possible methods to remove this approximate degeneracy, which would occur already in the simpler case of orbit determination for a spacecraft orbiting a planet with a well known orbit.

We conclude that it is possible to solve, simultaneously with the initial conditions $\mathbf{s}_i, \dot{\mathbf{s}}_i$ for each arc, for two ''synthetic'' observations of Mercury at the reference time t_i. Then ΔR_i and $\Delta\dot{R}_i$ can be used, in the second-step fit, as observations essentially of the same nature as the radar range and range rate data points, with the non-negligible advantage that the ''radar bounce point'' is the center of mass of the planet and is not subject to errors due to the topography of the planet.

The second step fit, the *PN corrector*, has the range $R(t)$ and range rate $\dot{R}(t)$ as observables, although each ''observation'' actually corresponds to the output of a fit with all the tracking data of one arc. The parameters to be determined are the corrections to the initial conditions of Mercury $\Delta\mathbf{M}_0 = \Delta\mathbf{M}(t_0)$ and $\Delta\dot{\mathbf{M}}_0 = \Delta\dot{\mathbf{M}}(t_0)$ at a single *reference time* t_0 [63]; analogous corrections $\Delta\mathbf{E}_0$ and $\Delta\dot{\mathbf{E}}_0$ for the initial conditions of the Earth; the mass of the Sun multiplied by the universal gravitational constant $M_0 = GM_\odot$; the PN parameters we are interested in determining; the change of the dynamical oblateness of the sun $\delta J_{2\odot}$ (with respect to the standard value 2×10^{-7}). The exact list of PN parameters can be changed, depending upon the assumptions (i.e., preferred frame parameters may or may not be included), but all the other parameters are needed. Note that a change in the Earth-Mercury range ΔR_i can be the result of a change in the orbit of Earth as well as of a change in the orbit of Mercury [64]: the orbit of our planet is by no means well enough determined by the presently available measurements and theories.

On the contrary, the orbits of the other planets are well determined enough, taking into account the weak coupling with the orbits of Mercury and Earth. The masses of all the planets (including Earth) are determined well enough by the tracking of spacecraft and/or by planetary perturbation theories (with the case of Jupiter being of principal importance, e.g. [65]). The case of the asteroids will be discussed in Sec. V. All these parameters do not need to be part of the adjustment, thus, if the number of PN parameters we are including in the solution (including $\delta J_{2\odot}$) is p, there are $13+p$ parameters to be determined.

An approximate rank deficiency of order 3 is obvious, resulting from the full rotation group applied to the orbits of Mercury and Earth. The symmetry would be exact if there were only the Sun, Earth and Mercury, and $J_{2\odot}$ was zero. Because of the coupling with the other planets, if the orbits of the other planets are kept fixed (as read in the JPL ephemerides), the symmetry is broken but only by an amount containing the small parameter ϵ, where ϵ is the relative size of the mutual perturbations by the other planets on the orbits of Earth and Mercury (with respect to the attraction by the Sun), such as the Roy-Walker parameters [61,62]. It is also broken by an amount containing the factor $J_{2\odot}$ because of the asphericity of the Sun, while the relativistic perturbations are also spherically symmetric (apart from the preferred frame effects).

Thus it is necessary to constrain the rotations of the planetary initial conditions. However, the approximate rank deficiency is of order 4 [66], and this is due to another symmetry which would be exact if only the Sun, Earth and Mercury were present. Suppose we change all lengths by a factor λ, all masses by a factor μ and all time intervals by a factor τ. By the method of similarities [67], if these factors are related by $\lambda^3 = \tau^2\mu$ (Kepler's third law) then the equations of motion of the gravitational 3-body problem are unchanged. We can assume $\tau = 1$, because there are accurate definitions of time scales based upon atomic clocks. If we have the mass of the Sun among the parameters, by rescaling it by $\mu = 1 + \Delta\mu$ (and keeping the mass ratios fixed) we can rescale the initial positions and velocities (by $\lambda \simeq 1 + \Delta\mu/3$). This is also expressed by the well known fact that it is not possible to solve simultaneously for the mass of the Sun and for the value (in terrestrial units, such as km) of the astronomical unit.

Since the coordinates of the other planets, as read from the JPL ephemerides, cannot be rescaled, the exact similarity symmetry becomes an approximate symmetry, with small parameters containing again the Roy-Walker small parameters (also the relativistic perturbations do not scale as the Newtonian attraction). Nevertheless we need to remove the cor-

responding approximate rank deficiency. This can be done in two ways: either by removing the mass of the Sun from the list of parameters, or by constraining the scale of the system by fixing some length.

The removal of all the approximate rank deficiencies of the PN corrector can be done in several different ways. We have selected as more convenient the following: we have removed all three components of $\Delta\mathbf{E}_0$ from the list of parameters to be adjusted, and we have constrained $\Delta\dot{\mathbf{E}}_0$, $\Delta\mathbf{M}_0$ and $\Delta\dot{\mathbf{M}}_0$ in such a way that rotations around the unit vector $\hat{E}_0$ are not allowed. Thus we have fixed the length $E_0 = |\mathbf{E}_0|$, making rescaling impossible. The method to constrain the parameters to inhibit a rotation, by adding one *a priori observation*, is described in Ref. [55]. Thus we are solving for $10+p$ parameters with one constraint, equivalent to a free solution with $9+p$ parameters.

Additional constraints (in the space of parameters to be solved with the PN corrector) can be optionally added. As we will see in Sec. IV, the most important one is the Nordtvedt relation [13,37,38]

$$\eta = 4\overline{\beta} - \overline{\gamma} - \alpha_1 - \frac{2}{3}\alpha_2, \tag{12}$$

which is justified if we assume that gravitation must be described by a metric theory. The technique to apply this constraint to the PN corrector least square fit is the same discussed above, by adding one *a priori* observation. It is also possible to assume that there are no preferred frame effects, that is to constrain $\alpha_1 = \alpha_2 = 0$. As we will see in Sec. IV, we have tested the sensitivity of our results with respect to these varying assumptions.

C. The superior conjunction experiment

As discussed in Secs. II A and II B, the PN parameter γ appears both in the equations of motion for Mercury (and Earth) and in the equations for radio wave propagation. However, these two effects change with time in a very different way. The changes in the orbit of Mercury undergo oscillations with periods of the order of the orbital and synodic periods, and have also a secular component (accumulating linearly with time); the effects over a few days are very small. On the contrary the light propagation delay depends quite sharply upon the Sun-Mercury angle as seen from Earth, when this angle is small, with Mercury beyond the Sun (this condition is called *superior conjunction*), as can be seen from Eq. (11) and from Fig. 1.

Thus it is possible to devise a *superior conjunction experiment (SCE)* using only the spacecraft tracking data over a time span of a few weeks around the epoch of a superior conjunction, and solving for a parameter γ_2 appearing in Eq. (11), as if it was a logically different PN parameter from the γ_1 appearing in the equations of motion Eq. (2). That is, the data from the entire mission are used to solve for γ_1, and the orbit of Mercury obtained from this solution is used as a reference orbit for the SCE. Of course $\gamma_1 = \gamma_2$ and this constraint must be used in the final results. This can be done in two ways. One method is to include in the runs of the PN corrector an *a priori* knowledge of γ_1, introduced as *a priori* observation, which is not based upon previous work but upon the output of the SCE, i.e., is on the knowledge of γ_2. The second method, applicable only if the information available on γ_2 is significantly superior to the one on γ_1, is to remove γ from the list of parameters to be solved by the PN corrector, and to use directly the results on γ_2 as results on γ. The choice between these two methods is discussed in Sec. IV B.

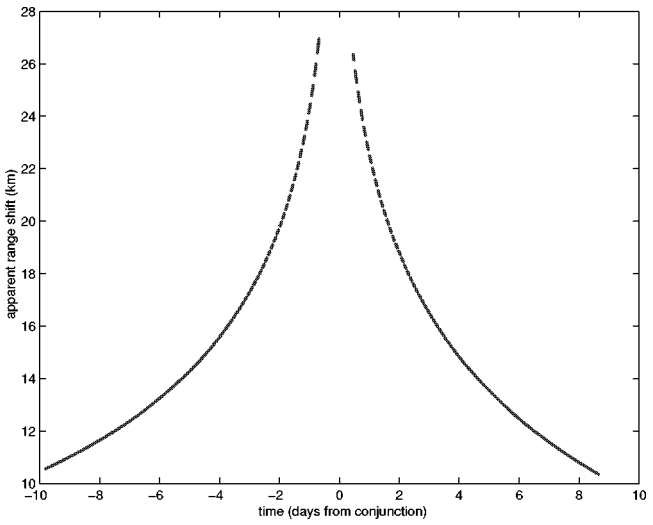

FIG. 1. The total sensitivity of the light propagation delay between a ground station and a Mercury orbiter to the value of γ (here we have assumed the GR value $\gamma=1$) as a function of time (in days) near the best superior conjunction with the Sun. Here the light propagation delay is represented in km, that is, as an increase in the distance to Mercury with respect to the distance along a flat spacetime. The gap in the data corresponds to the time interval during which the radio waves would be passing at less than 3 solar radii; the shorter interruptions are due to occultations of the satellite behind Mercury.

Since only a short span of data is used, for the SCE it is not necessary to resort to the two step fit described in Secs. III A and III B: γ_2 is just added to the list $\mathcal{G}$ of global parameters to be solved in the multiarc fit. The only tricky point is what should be done about the corrections to the orbit of Mercury, $\Delta R_i, \Delta\dot{R}_i$, appearing in the solution for the few arcs included in the SCE. Logically they should not be included, that is they should be constrained to be zero, since the orbit of Mercury has been already corrected. However, we need to ensure that the errors in the measurement of range, which is affected by a comparatively large systematic error, has a zero mean. For this purpose we also add a single, constant, ΔR correction to the set of global parameters $\mathcal{G}$. (The same could be done with a single correction $\Delta\dot{R}$, but this is less important because the range rate is not assumed to have large long term systematics; see Sec. IV A).

IV. THE EXPERIMENT SIMULATIONS

Having established, in the preceding two sections, a suitable theoretical and mathematical framework, we can now describe the simulation of the BepiColombo relativity ex-

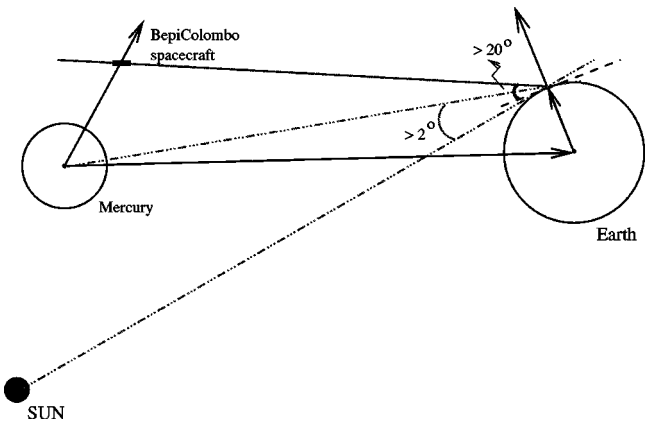

FIG. 2. Geometry of the system, given by the ground station, Mercury and the BepiColombo spacecraft. The visibility conditions from the ground station (elevation of the spacecraft larger than 20°) and the limiting Sun-Mercury angle are shown.

periment and present its results. Essentially we need to discuss the assumptions and results of the PN corrector: as it is clear from Sec. III B, the input for this second-step fit is a part of the output from the simulation of the gravimetry experiment of the same mission, which is described in Ref. [33]. Thus we begin in Sec. IV A by briefly recalling the assumptions on the data volume and error models used in the gravimetry simulation, and present the accuracies achieved, as a result of these assumptions, in the determination of the corrections ΔR_i, $\Delta \dot{R}_i$ to the orbit of Mercury.

In Sec. IV B we discuss the determination of γ, which turns out to be essentially the outcome of a suitable SCE. In Sec. IV C we describe the setup for the PN corrector, solving for most PN parameters and using the data from the entire mission, that is the observations of the orbit of Mercury over an entire year. In the same section we list the *a priori* information on the PN parameters we have used, which corresponds to an assessment of the current level of knowledge (based upon the references we have found). Finally Sec. IV D presents the results on all the other PN parameters (beside γ).

A. Assumptions

The assumptions in our simulations of the BepiColombo radio science experiment are described in Ref. [33], Section 2. Note that these assumptions are consistent with the ''official'' mission design as described in [30]. In short, we assume a mission with one year of operations in orbit around Mercury (no extended mission) in a 400×1500 km polar orbit. We assume a single ground station with Ka-band tracking capability. In the simulation, the station is located in Perth, Australia, where the ESA has a tracking station for which an upgrade to Ka-band is planned. The orbital and tracking geometry of BepiColombo is shown in Fig. 2. Basically, on board the spacecraft, the instruments used for the relativity experiment are the Ka-band transponder and the accelerometer.

Range rate measurements are taken continuously (one data point every 20 s) whenever the spacecraft is visible from the ground station: this results in data taken only over about 26% of the time. The observing sessions are controlled by the visibility of Mercury above the horizon at the station, with gaps resulting mainly from occultation by Mercury. Another visibility condition results from the Sun-Mercury angle as seen from Earth: in the full year simulation we have assumed that no data are taken when this angle is less than 2°. On the contrary we have assumed that for a time span of 20 days around the most favorable superior conjunction the observations are performed from three ground stations, all with Ka-band tracking capabilities, and down to a Sun-Mercury angle of 0.7°; these data are used only in the SCE.

The range data are taken within the same intervals of visibility, but only over intervals of 2 min every 15 min (this is to avoid reducing the bandwidth of the downlink). However, for the superior conjunction experiment the range data are taken continuously. The accelerometer is assumed to be on all the time (indeed, to turn off the accelerometer would be a mistake, given the problems with the thermal transients).

The error model for the range and range rate tracking is described in Ref. [29], the one for the accelerometer in Ref. [28]. The main property of these error models is that they contain not only noise, but also systematic errors. This property needs to be exploited to generate, with the simulations, an assessment of the systematic as well as the random error in the final results, that is in the estimated values of the PN parameters.

The main systematic effects in the tracking data are apparent in Fig. 4 of Ref. [33]. The random components result in a rms error of 10 cm for the range and 1.8×10^{-3} cm/s for the range rate. The main systematic effect is given by a nonlinear drift of $50\sin(\pi/2\times t/365)$ cm, where t is the time from the beginning of the Mercury orbiting phase in days. (This drift is assumed to represent the degradation with time of the on-board transponder, for which an absolute calibration is difficult.)

The error components of the accelerometer measurements acting over intermediate time scales (10^3 to 10^4 sec), shown in Fig. 5 of Ref. [33], model the temperature change of the accelerometer sensing units. Longer term drifts matter much less, because calibration constants can be determined for each arc (they are added to the set of local variables ℓ_i). The main effect of the accelerometer inexact measurements is to degrade the orbital solution, at a level depending upon the duration of the arc. If we use an arc length corresponding to one observing session from the ground station (with a duration depending upon the season, but averaging 8 h), then the systematic errors in the arc initial positions are of the order of 1 m, but the errors in the corrections to Mercury's center of mass have a rms of 1.8×10^{-3} cm/s^2 for $\Delta \dot{R}_i$. For ΔR_i there is a short term noise with the rms 4.5 cm superimposed to a systematic drift which of course exactly mimics the systematic range noise of $50\sin(\pi/2\times t/365)$ cm. Indeed there is no way to differentiate, by range measurements, a calibration drift from a displacement of Mercury along the line of sight.

The conclusions from this discussion can be summarized as follows. First, the accelerometer measurement error does

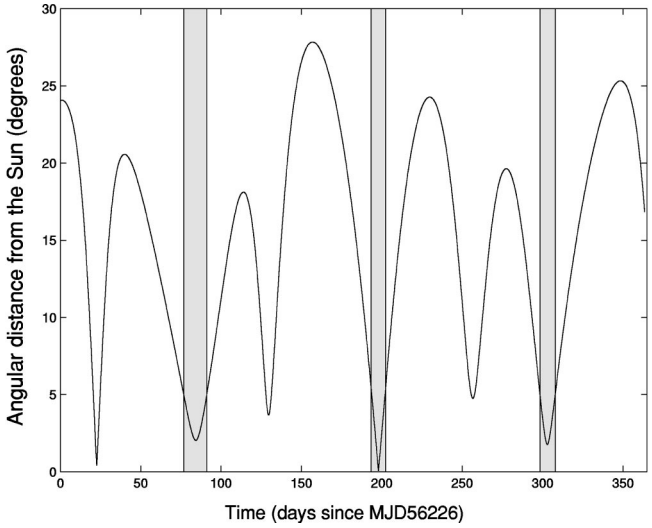

FIG. 3. The angular distance of the BepiColombo spacecraft from the center of the solar disk (in degrees) vs time (in days) since the expected injection into the mercurycentric orbit, over the nominal mission duration of one year. Three superior conjunctions are marked by shaded strips (when the elongation is less than 5°). The most promising conjunction occurs on day 197.7 of the mission, when the spacecraft will actually be occulted by the solar disk. The other two superior conjunctions have minimum elongation 1.75° and 2°, respectively, thus they can contribute complementary, but not essential, data.

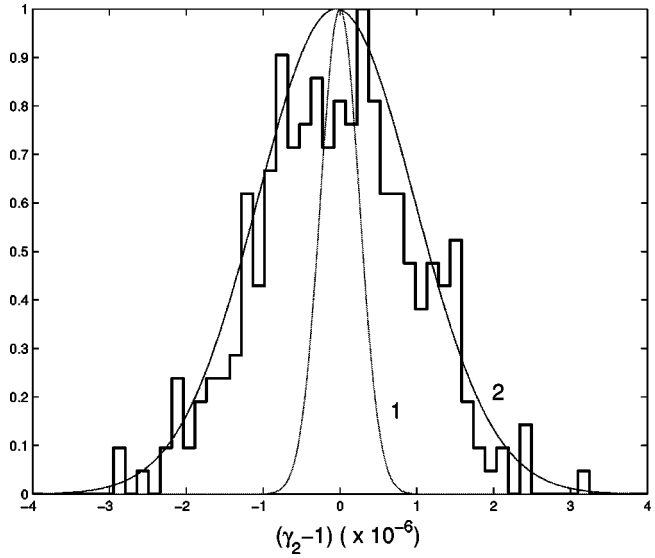

FIG. 4. SCE solution for γ_2: (i) the light curve 1 corresponds to the formal solution, (ii) the histogram shows the actual distribution of the 300 results from our simulations, and (iii) the light curve 2 indicates the Gaussian approximation of the solutions (for the sake of comparison, all data normalized to unity). Note the factor $\simeq 4$ between the actual rms of the results for γ_2 and the formal rms.

not affect very much the determination of the synthetic observations of the orbit of Mercury. Second, the systematic errors in ranging are the main source of systematic errors in the relativity experiment. Third, the range rate measurements, and their error model, do not matter very much for the relativity experiment (while they contain most of the information for the gravimetry experiment). This last conclusion arises from the simple fact that information on the range rate accurate to a few 10^{-3} cm/s, if used to estimate range changes, is more accurate than range measurements accurate to a few 10 cm if the time scale is just a few 10^3 seconds (e.g., over an orbital period of the satellite, 2.3 h), but less accurate if the time scale is months. The intermediate case of the SCE, where the time scale is a few days, is not obvious. Although this is a simplification, we can roughly say that the orbit of the spacecraft around Mercury is determined by the range rate measurements, the orbit of the planet is determined by the range measurements. (We have nevertheless used both the range and range rate data both in the multiarc fit and in the PN corrector).

B. Determination of γ

The circumstances for possible superior conjunction experiments, given the assumptions on the mission plan of the BepiColombo Planetary Orbiter from Ref. [30], are shown in Fig. 3. There is one especially good superior conjunction, in which the tracking data can be taken from radio waves passing as close to the Sun as allowed by the plasma noise compensation procedure, supposedly down to ≈ 3 solar radii.

We have simulated such a SCE with the assumption that three ground stations, well distributed in longitude, would provide a continuous tracking (apart from occultations of the satellite behind Mercury). Thus the dataset is not naturally subdivided into arcs: we have selected an arc length of 80000 s, thus formed 20 arcs, 10 before and 10 after the $\simeq 1$ day interruption of the tracking due to an elongation less than 0.7°. Then we have performed a multiarc solution with local parameters amounting only to the satellite initial conditions and to accelerometer calibrations, and with global parameters γ_2 and a single, constant ΔR (to absorb the average, over the time span of 20 days, of the range calibration shift). Note that we are assuming that both the orbit of Mercury (apart from a constant shift in distance from Earth) and the gravity field of Mercury are known, supposedly from the processing of the rest of the data. In the simulation we have assumed that the orbit of Mercury is according to GR, and also $\gamma_2 = 1$.

The main advantage of such a SCE is to reduce the influence of the systematic range error, because its variation from a constant over $\simeq 20$ days is less than 5 cm, and thus is less than the random error in the ΔR_i (if these were determined as local parameters). However, it is not the case that there are no systematic effects: also the accelerometer measurement error has some influence, and we need to assess how much the systematics degrade the result with respect to the formal, random error as expressed by the covariance matrix. Thus we have performed 300 simulations of the SCE, with different seeds for the random number generators used to simulate the random error component of the range, range rate, and accelerometer measurements. Figure 4 shows the histogram of the values of $\gamma_2 - 1$ derived in these 300 tests compared with the

Gaussian corresponding to the rms of γ_2 from the covariance matrix of any one of them.

The conclusion is that the formal uncertainty, with rms 2.5×10^{-7}, gives an illusory precision and should be replaced, in a realistic assessment of the achievable accuracy, by a far larger value, which could be 2×10^{-6} (this corresponds to $2\times$ rms of the distribution of the results shown in Fig. 4).

We have tested the intuitive idea that the range rate measurements contribute very little information to the relativity experiment even in the SCE setting, by running a simulation with the range observations strongly underweighted with respect to the range rate ones. The result was that the uncertainty of γ_2 increased by more than one order of magnitude, and this already at the formal level. We conclude that the range measurements are the critical ones, and that the main sources of the systematic error in γ_2 must be the systematic drift in range and the accelerometer measurement error.

For comparison purposes, we need to cite the results which could be obtained by including $\gamma=\gamma_1=\gamma_2$ among the parameters to be solved in a full PN corrector simulation with one year of data. We have indeed tried this method too, although we do not discuss elsewhere the results, precisely because they were not as good as the ones obtained by the SCE. Depending upon the assumptions on the Nordtvedt constraint we can have errors in γ, from a solution not using a SCE, ranging between 1×10^{-5} and 1.5×10^{-5}. These results are strongly affected by systematic errors, that is the formal uncertainties are significantly less.

We can now draw the conclusions on how the results of the superior conjunction experiment should be inserted in the global solution for all the PN parameters (and other solar system model constants). The solution of combining the information on γ_2 from the SCE and the information on γ_1 from the one year solution has a problem of weight balancing. Indeed the information from both solutions should be combined by using weights derived from the actual errors, not from the formal errors. Anyway the contribution from the one year solution to the combined result for γ would be minor. Therefore we have adopted the simpler solution, which is to assume the solution for γ_2 obtained from the SCE, with the realistic error estimation given above as the final result on γ and to remove altogether γ from the set of parameters to be solved in the PN corrector. In this way the information on $\gamma=\gamma_2$, as obtained from the SCE, is correctly employed to strengthen the solution for the other parameters. We have tried to obtain a final solution in many different ways, and this method indeed gives the best solution for all the PN parameters.

C. The one year simulations

Having reached the conclusions of Sec. IV A from a (small) number of multiarc fits, we can now simulate a large number of PN corrector runs. First, we assume that GR holds exactly (and the other solar system parameters, including $J_{2\odot}$ and $GM_\odot$, have their nominal value). For each run of the PN corrector, we generate values of $\Delta R_i, \Delta\dot{R}_i$, one for each arc, according to the error model described above, with always the same systematic component for range and the random components in both range and range rate from a random generator of Gaussian distributions. We typically perform 2000 runs for each simulation with different assumptions (e.g., with and without the Nordtvedt constraint, with and without preferred frame parameters). Then we perform another 2000 runs with no systematic error component, to show by comparison the relevance of the systematic component. The output is then presented in a plot showing, for each parameter being solved, (1) the histogram of the results from the simulations with random error only, (2) the Gaussian distribution predicted by the covariance matrix, (3) the histogram of the results from the simulations with systematic as well as random errors, (4) the Gaussian distribution best fitting to the previous histogram: note that the average is, in most cases, significantly different from zero, thus there is a bias in the results (on the contrary the rms of the results with systematic error is not significantly different from the value predicted from the covariance matrix).

In Table I we list the present knowledge of the PN parameters, as we have found in the literature. This information has two purposes. On one hand, we use it as a benchmark to evaluate the increase in accuracy achievable with the BepiColombo relativity experiment. On the other hand, this information is used as *a priori*, e.g. an ''observation'' $\beta=1$ with weight corresponding to a rms of 3×10^{-3} is added. This helps in stabilizing the solution, in particular in the presence of high correlations, but is a legitimate way to combine the previous with the current information.

TABLE I. Current constraints on the PN parameters. Note that these are rms results from the corresponding least square fits. Compare with the possible results from the BepiColombo mission given in Table II.

Parameter	Value	Primary reference
$\overline{\beta}$	3×10^{-3}	Ref. [10][a]
$\overline{\gamma}$	1.7×10^{-3}	Ref. [18][b]
η	10^{-3}	Ref. [17]
$d(\ln G)/dt$	4×10^{-12}	Ref. [70][c]
α_1	3×10^{-4}	Ref. [71][d]
α_2	3×10^{-4}	Ref. [13][e]

[a]If the best value of $\overline{\gamma}$ parameter is combined with the lunar laser ranging (LLR) solution for η one may obtain a better value for $\overline{\beta}$, notably 6×10^{-4}, Ref. [17].

[b]Though a combination of a large number of VLBI observations may eventually yield a better solution, e.g., Ref. [68], we conservatively adopt the best value from a single experiment (not relying on a statistical decrease of the formal uncertainty).

[c]Recent reanalysis of the LLR data may have the capability of decreasing the limit to 10^{-12} as quoted in Ref. [69].

[d]LLR and binary pulsar data result in comparable values, Ref. [72] and Ref. [73].

[e]Here we intentionally use the best *experimental* constraint on this parameter. Nordtvedt in Ref. [74] gives a plausible, but *theoretical argument* for much better value of 4×10^{-7}, which our data could confirm experimentally.

TABLE II. A summary of the results from our experiments. The numbers in parentheses indicate exponent of basis 10 by which the result is multiplied.

	$\alpha_1=\alpha_2=0$				All parameters				
	Expt. A (non-metric)		Expt. B (metric)		Expt. C (non-metric)		Expt. D (metric)		
Parameter	rms	Real.	rms	Real.	rms	Real.	rms	Real.	Parameter
$\overline{\beta}$	6.7 (−5)	**2.2 (−4)**	7.5 (−7)	**2.0 (−6)**	7.6 (−5)	**5.6 (−4)**	9.2 (−7)	**7.0 (−6)**	$\overline{\beta}$
α_1	–	–	–	–	7.3 (−7)	**8.7 (−6)**	7.1 (−7)	**7.8 (−6)**	α_1
α_2	–	–	–	–	2.1 (−7)	**1.6 (−6)**	1.9 (−7)	**1.1 (−6)**	α_2
η	4.4 (−6)	**1.5 (−5)**	3.0 (−6)	**7.9 (−6)**	5.1 (−6)	**4.5 (−5)**	3.3 (−6)	**2.0 (−5)**	η
$d(\ln G)/dt$	4.0 (−14)	**5.2 (−13)**	3.9 (−14)	**5.3 (−13)**	4.0 (−14)	**4.7 (−13)**	3.9 (−14)	**5.2 (−13)**	$d(\ln G)/dt$
δJ_2	7.9 (−9)	**2.8 (−8)**	2.4 (−10)	**2.1 (−9)**	8.9 (−9)	**6.2 (−8)**	6.2 (−10)	**4.8 (−9)**	δJ_2
μ	1.9 (−12)	**5.9 (−12)**	3.3 (−13)	**1.0 (−12)**	2.1 (−12)	**1.5 (−11)**	4.1 (−13)	**1.0 (−12)**	μ

D. Results

We have performed a large number of tests with the PN corrector, but the main simulated experiments are four, resulting from the combinations of two binary choices. We did include the constraint corresponding to the Nordtvedt relation [Eq. (12)] in experiments B and D, while experiments A and C correspond to non-metric theories (η is solved as a parameter independent from the others). We did assume no preferred frame effects in experiments A and B, while we solved for α_1 and α_2 in experiments C and D.

All the results are summarized in Table II. For each of the parameters we give (i) the formal rms uncertainty from the covariance matrix of the solution, and (ii) a ''realistic'' level of accuracy (bold) at which this parameter can be determined from the experiment. This latter accounts for all systematic effects in the observation model (plus the random-noise component) and was defined as a mean value of this parameter from the 2000 simulations with systematic effects plus $2\times$ rms of the formal uncertainty (this amounts to $\simeq 93\%$ confidence level of this formal solution). Note that γ is not included in the table because the results for γ_2 are to be used. Thus the rms for γ is 2.5×10^{-7}, the formal rms of the SCE, and a realistic error estimate is given by $2\times$rms of the histogram of Fig. 4, which is 2×10^{-6}. We are not including in this case a bias term because there is no obvious bias in the histogram.

1. The rate of change of G

The least satisfactory result is the one for the rate of change of the gravitational constant G. As it is clear from Table II, in all the four experiments the systematic errors are one order of magnitude larger than the formal ones. This can be understood as follows.

As is apparent from Fig. 5, this parameter is the only one for which the bias is so much dominant with respect to the random component of the error. The main orbital signature of a secular change of gravity with time is that Mercury's mean motion has a linear drift. This results in an accumulated along track displacement, which can be estimated by a simple formula to be $\simeq 15$ cm after one year for $d(\ln G)/dt = 10^{-13}$. Thus the quadratic component of the range calibration drift aliases almost perfectly with this signature, and this

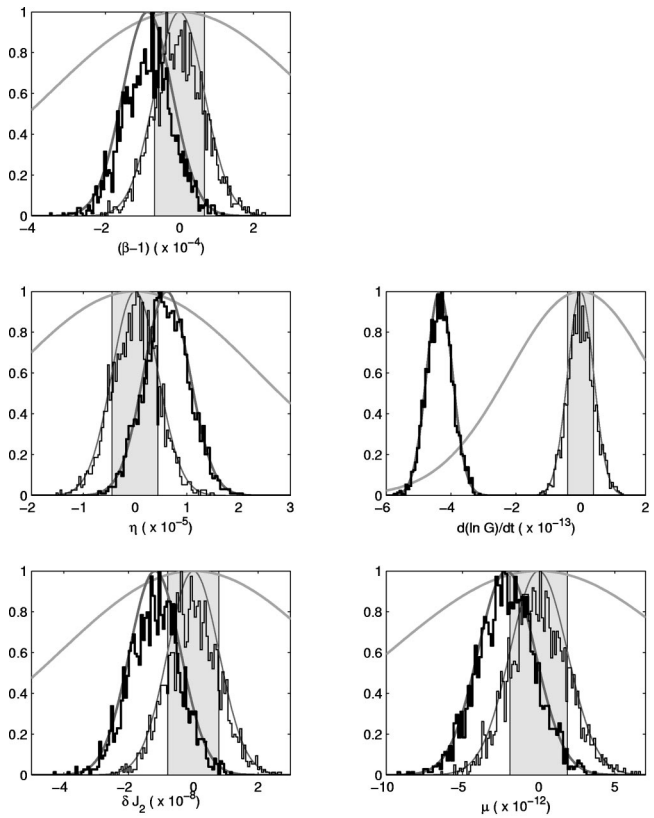

FIG. 5. Distribution of the results for the PN and solar parameters from the 2000 simulations of the one-year orbital arc of Mercury, experiment A. The preferred frame PN parameters are not considered and the Nordtvedt parameter η is assumed independent. The distribution histograms are normalized to unity. The light histograms correspond to the simulations where systematic effects in observations were removed and the noise contains only a random component; the bold histograms correspond to the simulations with the complete noise model (systematic and random). The smooth overlapping curves are formal Gaussian distribution from the covariance matrix of the solution (the shaded area indicates formal rms of the unbiased solution). The wide Gaussian curve is a formal solution, with only a random noise in the observations having rms of 25 cm, namely half of the principal systematic effect in range. Note the seriously corrupted solution of the $d(\ln G)/dt$ parameter due to systematic effect in the realistic solution.

TABLE III. Formal results for the PN and solar parameters from the analysis of one year Mercury's orbital data. rms means standard deviation from the diagonal terms in the covariance matrix. The numbers in the triangular area are the correlation coefficients (rounded to 2 digits) from the off-diagonal terms in the covariance matrix. The correlations larger than 90% are highlighted in bold.

Parameter	rms	$\overline{\beta}$	η	$\frac{d(\ln G)}{dt}$	δJ_2
$\overline{\beta}$	6.7 (-5)	–			
η	4.4 (-6)	-0.73	–		
$d(\ln G)/dt$	4.0 (-14)	-0.23	0.16	–	
δJ_2	7.9 (-9)	**1.00**	-0.74	-0.25	–
μ	1.9 (-12)	**0.98**	-0.79	-0.27	**0.99**

explains in a qualitatively satisfactory way the systematic error for $d(\ln G)/dt$.

Unfortunately, the currently known constraint is just one order of magnitude larger than the accuracy of our experiment as planned now. Moreover, we are aware that the lunar laser ranging measurements are going on, and they are believed to be capable of reaching an accuracy of 10^{-12} well before the time when BepiColombo will be around Mercury. The conclusion is that the limitation to the accuracy in $d(\ln G)/dt$ is due essentially to the assumed drift in the range calibration. Thus the only way to obtain a result superior to that of other methods would be to significantly improve the stability of the ranging transponder.

2. Non-metric theories

The main problem with the results of experiment A (and C) is the strong correlation between β and $J_{2\odot}$, as is apparent from the covariance matrix obtained in the least squares fit (see Table III). The main orbital effect of β is a precession of the argument of perihelion, which is a displacement taking place in the plane of the orbit of Mercury; $J_{2\odot}$ affects the precession of the longitude of the node, i.e., generates a displacement in the plane of the solar equator [75]. The angle between these two planes is only $\epsilon = 3.3°$ and $\cos\epsilon = 0.998$, thus it is easy to understand how the correlation between β and $J_{2\odot}$ can be 0.997. The correlations between β, $J_{2\odot}$ and the mass of the Sun (actually, the scale factor, which could be expressed as the value of the astronomical unit in km) are also critical.

There is no way to decrease this correlation without observing (with equivalent accuracy) some other celestial body moving around the Sun in an orbit with a quite different inclination and/or semimajor axis (e.g., [76]). The effect of such a strong correlation is illustrated in Fig. 6: the observations of the orbit of Mercury can constrain very well some linear combination of β and $J_{2\odot}$, but there is a "weak direction" along which another combination of the same parameters is only weakly constrained. When the relationship of Eq. (12) is used as a constraint, the confidence region for these two parameters collapses to a less elongated and much smaller region. In fact the smaller confidence region of the lower plot in the figure is contained in the intersection of the longer confidence region with the strip parallel to the $J_{2\odot}$ axis representing the knowledge of β as determined from the value of η. The conclusion is that the best way to solve for β (and $J_{2\odot}$, which is interesting by itself) is to use Eq. (12); of course this is an assumption, hence experiment B (and D) cannot be considered as an experimental test of the hypothesis that gravity is described by a metric theory.

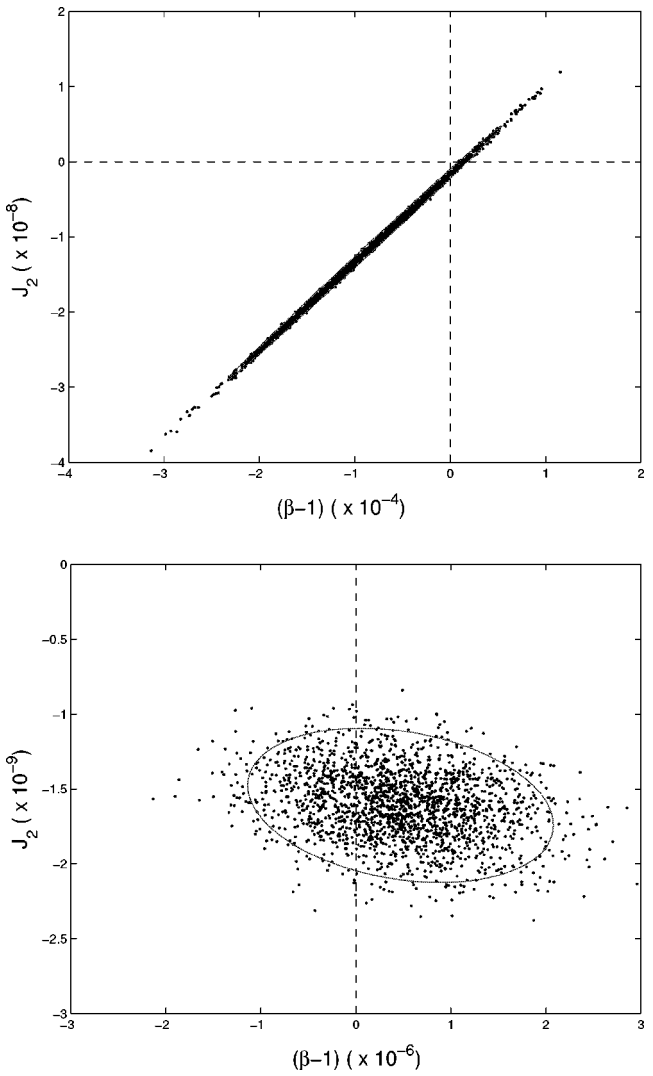

FIG. 6. Values for $\overline{\beta}$ and $\delta J_{2\odot}$ as solved from 2000 simulations of Mercury's one year orbit. The full error model for the observations (containing both the random and systematic components) is assumed. The upper plot is from experiment A, where the Nordtvedt parameter η is independent, while the lower plot is from experiment B, where η is constrained to be equal to $4\overline{\beta} - \overline{\gamma}$ (no preferred frame effects assumed). The large correlation (99.7%) decreases the quality of the solution of both parameters in experiment A, while in experiment B the correlation between these two parameters is suppressed and a much more accurate solution is obtained. The light curves indicate the formal 90% confidence level as deduced from the respective covariance matrices.

3. Metric theories

In the experiment B, the Nordtvedt parameter η was assumed to be linked to the other PN parameters through the

TABLE IV. Formal results for the PN and solar parameters from the analysis of one year Mercury's orbital data, experiment B. The conventions are the same as in Table III. In this solution, η is forced to be equal $4\overline{\beta}$. Correlations larger than 90% are highlighted in bold.

Parameter	rms	$\overline{\beta}$	η	$\frac{d(\ln G)}{dt}$	δJ_2
$\overline{\beta}$	7.5 (-7)	-			
η	3.0 (-6)	**1.00**	-		
$d(\ln G)/dt$	3.9 (-14)	-0.01	-0.01	-	
δJ_2	2.4 (-10)	-0.26	-0.26	-0.41	-
μ	3.3 (-13)	-0.56	-0.56	-0.21	0.71

Nordtvedt relation $\eta=4\overline{\beta}-\overline{\gamma}-\alpha_1-\frac{2}{3}\alpha_2$ (this is used as a constraint in the least squares fit). Since $(\overline{\gamma},\alpha_1,\alpha_2)$ are kept constant in this solution, the Nordtvedt relation used as constraint in this experiment is just $\eta=4\overline{\beta}$. As a result the covariance matrix, described by Table IV, has a correlation exactly 1 between β and η (these are not independent parameters at all), but the other correlations have been greatly reduced, especially the one between $\overline{\beta}$ and $J_{2\odot}$. Note that, on top of the uncertainty indicated in Tables IV and II, we should account for the effect of the uncertainty on γ_2 from the SCE, since in fact $\eta=4\overline{\beta}-\overline{\gamma}$ and $\overline{\gamma}=\gamma_2-1$.

The results from 2000 simulations with systematic range errors and 2000 with random errors only are shown in Fig. 7. The comparison with Fig. 5 and the values from Table II indicate a significantly better accuracy for all PN parameters but $d(\ln G)/dt$ (the quadratic systematic effect is the same). Even accounting for the effect of the 2×10^{-6} uncertainty on γ, η is anyway constrained to 10^{-5}. We can conclude that, within the framework of metric theories of gravitation, the PN parameters β,γ,η and the solar system model parameters μ, $\delta J_{2\odot}$ can be determined with significantly improved accuracy (two orders of magnitude better than the present knowledge). In some sense, this is the best solution, but it uses one additional assumption.

4. Preferred frame effects

The data from the BepiColombo relativity experiment can also be used to test the possible preferred frame effects, in particular by constraining the PN parameters α_1 and α_2. Experiment C is the same as experiment A but with α_1 and α_2 added to the list of parameters to be determined. From the data in Table II we can see that the accuracy on α_1 and α_2 is significantly better than the previous knowledge. The price is some degradation in the accuracy for η, β, $\delta J_{2\odot}$, μ. From the data on the left (and below the main diagonal) in Table V we can see that the high correlations between β, $\delta J_{2\odot}$ and μ, found in experiment A, are still present, thus the accuracy on these three parameters is not very satisfactory.

Therefore we have also run an experiment D in which we solve for α_1 and α_2, but also use the constraint $\eta=4\overline{\beta}-\overline{\gamma}-\alpha_1-\frac{2}{3}\alpha_2$. As a matter of fact $\overline{\gamma}$ is kept fixed, assumed to be determined from the SCE. From the data on the right (and above the main diagonal) in Table V we can see that the correlation between β and $\delta J_{2\odot}$, μ has been sharply decreased. The correlation between η and β is high, although not exactly 1, since β also depends upon α_1 and α_2 (indeed, the correlation with α_1 is rather high). From Fig. 8 and the data in Table II we can conclude that the accuracy is improved with respect to experiment C for η, β, $\delta J_{2\odot}$ and μ, while the accuracy for α_1 and α_2 is not much affected. If we compare experiment D with experiment B there is some degradation in the accuracy on β, η and $\delta J_{2\odot}$, which appears as the price to pay for testing the presence of preferred frame effects.

Note that the accuracy in the determination of the preferred frame parameters, especially α_1, depends upon the orientation of the present orbit of Mercury with respect to the assumed preferred frame direction. At present the line of apsides of Mercury is roughly orthogonal to the velocity of the solar system with respect to the cosmic microwave background, and this turns out to be an unfavorable configuration for the determination of α_1.

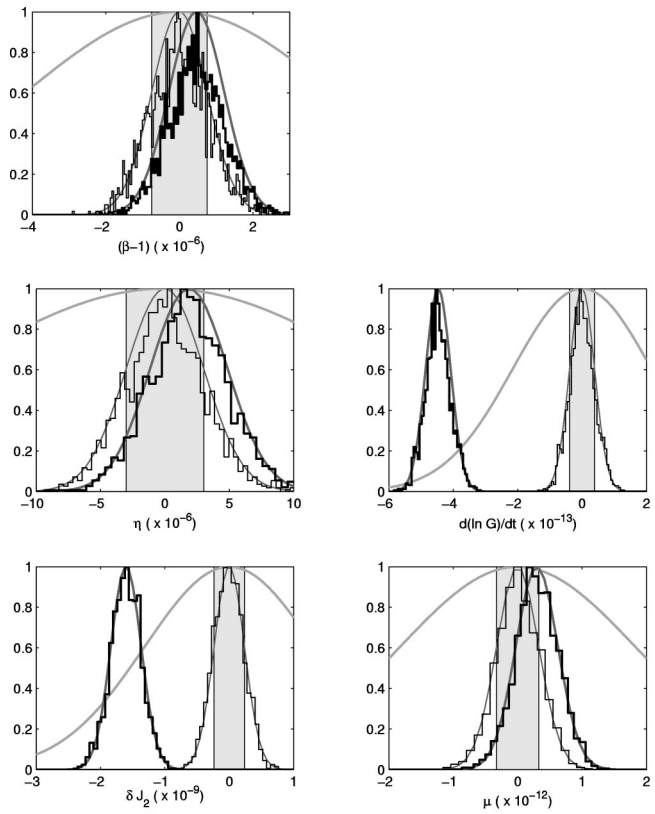

FIG. 7. The same as in Fig. 5, but for experiment B, assuming the relationship between η and β from Eq. (12). The correlation between $\overline{\beta}$ and $\delta J_{2\odot}$ is thus suppressed in this solution, and these parameters are determined with much better accuracy.

V. FUTURE WORK

There are of course some open problems, which deserve further investigations to be conducted between now and the scheduled launch window. The main problems are to make

TABLE V. Formal results for the PN and solar parameters from the analysis of one year Mercury's orbital data, experiments C and D. The data on the left and the subdiagonal correlations correspond to experiment C with η taken as independent parameter; the data on the right and the superdiagonal correlations correspond to experiment C where the Nordtvedt relation for η was used. Correlations larger than 90% are highlighted in bold.

Parameter	rms	$\overline{\beta}$	α_1	α_2	η	$\frac{d(\ln G)}{dt}$	δJ_2	μ	rms	Parameter
$\overline{\beta}$	7.6 (−5)	-	0.58	−0.04	**0.98**	0.03	0.46	−0.54	9.2 (−7)	$\overline{\beta}$
α_1	7.3 (−7)	−0.21	-	−0.02	0.43	0.06	**0.92**	−0.28	7.1 (−7)	α_1
α_2	2.1 (−7)	−0.43	0.07	-	−0.08	−0.11	−0.05	0.54	1.9 (−7)	α_2
η	5.1 (−6)	−0.75	0.44	0.28	-	0.03	0.31	−0.56	3.3 (−6)	η
$d(\ln G)/dt$	4.0 (−14)	−0.22	0.11	0.00	0.19	-	−0.09	−0.24	3.9 (−14)	$d(\ln G)/dt$
δJ_2	8.9 (−9)	**1.00**	−0.15	−0.44	−0.74	−0.23	-	−0.06	6.2 (−10)	δJ_2
μ	2.1 (−12)	**0.98**	−0.26	−0.33	−0.82	−0.27	**0.98**	-	4.1 (−13)	μ

sure that our observation model, our solar system dynamical model and the relativistic theories used are adequate to the extreme accuracy of the measurements.

The tracking of the BepiColombo main orbiter needs to be conducted from ground stations fully equipped for the Ka-band, with the electronic and thermo-mechanical stability corresponding to the expected measurement accuracy. The water vapor content of the atmosphere needs to be measured to account for tropospheric propagation delays. Interplanetary tracking to this accuracy had never been achieved until recently: the first tests of the new generation tracking system on board the Cassini spacecraft have demonstrated that, at least for range rate, the requirements assumed in this paper can be achieved and possibly exceeded [78]. An in depth analysis of the outcome of these experiments (and of other tests already planned) is required before the time of the BepiColombo experiment.

The parameters of the solar system model not solved in our fit, that is on the basis of the Mercury-tracking data, need to be known well enough not to introduce aliased effects in the relativity experiment. While the planetary masses should not be a problem, a source of concern is the unknown, or poorly known, masses of the asteroids. The perturbations on Mercury are negligible, but Earth is displaced by the short period perturbations of Ceres by $\simeq 3$ m; since the mass of Ceres is known only to about 5%, this effect alone is responsible for an uncertainty which is not negligible with respect to the accuracy of the range measurements. The cumulative effect of the $\simeq 100$ asteroids capable of perturbing Earth's orbit (over one year) by 1 cm or more is significant for our experiment [77], and for most of these asteroids only a very rough estimate of the mass is available. Thus the ongoing work to improve our knowledge of the mass of Ceres and the largest asteroids is important, and we need to assess the overall effect of these poorly modeled perturbations on the accuracy of the final results.

The accuracy of the BepiColombo relativity experiment is such that it reaches the threshold at which second post-Newtonian order effects become significant, e.g., some of these effects are discussed in Refs. [79] and [80]. We need to carefully investigate the possible effects of this class, and include in the model the ones which can affect the results.

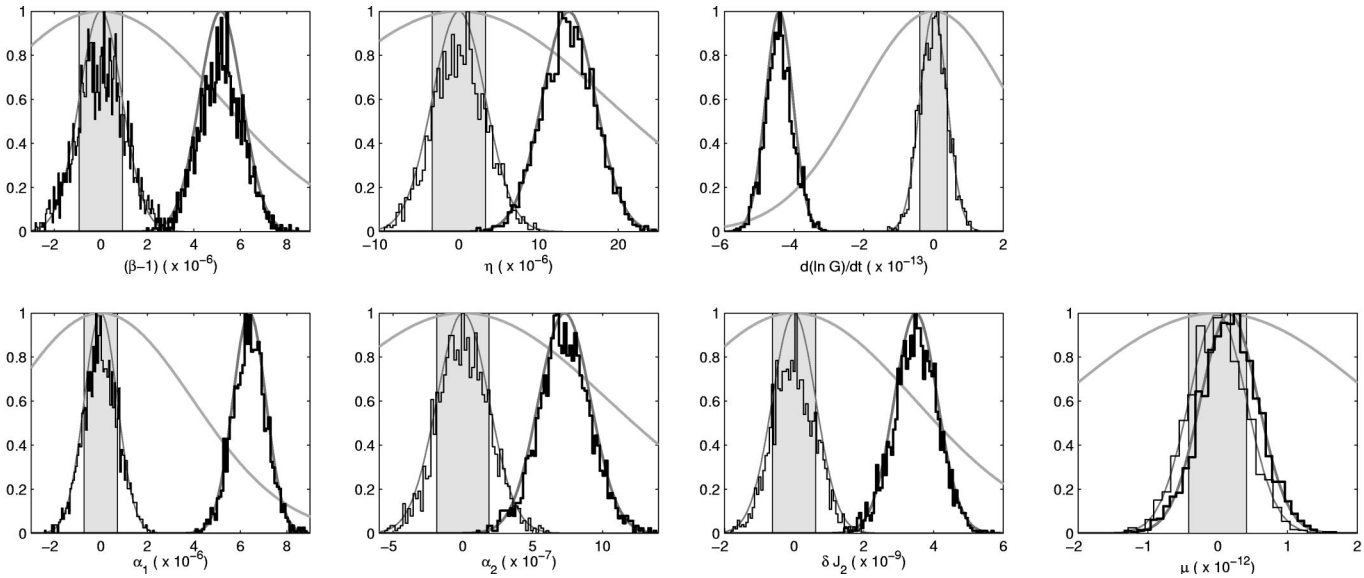

FIG. 8. The same as in Fig. 7, but here the preferred frame parameters α_1 and α_2 were included in the solution.

VI. CONCLUSIONS

We conclude by summarizing the results we have achieved.

(1) We have shown that the relativity experiment of the BepiColombo mission to Mercury is feasible as proposed. More exactly, the results on almost all the PN parameters (and $J_{2\odot}$) can represent a significant improvement (about two orders of magnitude) with respect to the current knowledge, provided the mission plan corresponds to the present baseline [30] and the instrument performances can be assumed to be as expected now (as described in Refs. [28] and [29]).

(2) We have identified the range drift (in the calibration of the on board transponder) as the main limitation to the accuracy of the results. In particular, this effect is responsible for the unsatisfactory results on $d(\ln G)/dt$, the only PN parameter for which it is possible to achieve only a small improvement (a factor $\simeq 2$) with respect to the accuracy expected to be available before the time of BepiColombo. To improve the results on $d(\ln G)/dt$ it would be desirable to have an extended mission, with up to two years in orbit around Mercury, but this is useful only if there is a good understanding of the behavior of the ranging transponder over two years [81].

(3) The performance of the Doppler measurements of range rate, and of the accelerometer measurements, do not appear to be critical for the relativity experiment (while they are critical for the gravimetry experiment, as described in Ref. [33]). They contribute essentially only to the random error component, which is secondary with respect to the systematic errors due to the range measurements.

APPENDIX: PLANETARY TEST OF SEP

In this Appendix we discuss in more detail the planetary test of the strong equivalence principle (SEP). Our approach is similar, but not identical, to that in Ref. [32], where the authors considered testing η from radar ranging to a Mars-landed transponder.

Testing any version of the equivalence principle means testing a hypothesis that the ratio of the gravitational M_i^g and inertial M_i masses is not a universal constant (e.g., 1), but depends on the composition of a given object (in this appendix we use the letters $i,j,\ldots$ for numbering the bodies in the planetary system). In the context of celestial mechanics, this means testing the orbital effects of the Lagrangian terms described in Eqs. (4) and (5) in Sec. II A. We are concerned with testing the strong equivalence principle, hence $\delta_i = \eta\,\Omega_i = \eta\,(E^{\rm grav}/Mc^2)_i$. Here Ω_i is a gravitational compactness factor; of course, among the solar system bodies the Sun has the largest value $\simeq -3.52\times 10^{-6}$. Testing the equivalence principle requires an experiment with at least three bodies: two objects falling in the gravity field of a third body. We consider a motion of a complete planetary system, but the principal bodies of interest are the Sun, Mercury, Earth and Jupiter. As in Ref. [32], our method principally tests whether bodies in the Sun-Mercury and Sun-Earth pairs fall with the same acceleration in the gravitational field of Jupiter.

We now focus on modifications of the planetary equations of motion due to the possible SEP violation. Assuming barycentric coordinates $\mathbf{r}_i$ of the ith body we have

$$\frac{d^2\mathbf{r}_i}{dt^2} = -G\sum_{j\neq i}\,[1+\eta(\Omega_i+\Omega_j)]\frac{M_j}{r_{ij}^3}\mathbf{r}_{ij}\quad , \tag{A1}$$

with $\mathbf{r}_{ij}=\mathbf{r}_i-\mathbf{r}_j$. A number of additional terms (including GR effects $\propto 1/c^2$) are neglected on the right-hand side of Eq. (A1). Assume the indexes span values $0,1,\ldots,(n-1)$ (for $n-1$ planets), with 0 meaning the Sun. Up to the neglected terms, the center of mass system is still defined by

$$\sum_{i=0}^{n-1} M_i\mathbf{r}_i = 0. \tag{A2}$$

This allows a suitable elimination of 6 variables, such as the position and velocity of the Sun. This reduction is obtained by introducing heliocentric coordinates $\mathbf{q}_i$: $\mathbf{q}_i=\mathbf{r}_i-\mathbf{r}_0$ for $i \geqslant 1$. The relative motion of planets around the Sun then satisfies

$$\begin{aligned}\frac{d^2\mathbf{q}_i}{dt^2} &= -G[1+\eta(\Omega_0+\Omega_i)]\frac{M_0+M_i}{q_i^3}\mathbf{q}_i \\ &\quad -\sum_{j\neq 0,i} G[1+\eta(\Omega_i+\Omega_j)]M_j\left(\frac{\mathbf{q}_{ij}}{q_{ij}^3}+\frac{\mathbf{q}_j}{q_j^3}\right) \\ &\quad -\eta(\Omega_0-\Omega_i)\sum_{j\neq 0,i}\frac{GM_j}{q_j^3}\mathbf{q}_j\,,\end{aligned} \tag{A3}$$

where $\mathbf{q}_{ij}=\mathbf{q}_i-\mathbf{q}_j$ [note that the indexes now span $1,2,\ldots,(n-1)$]. If compared with the traditional planetary equations of motion in heliocentric coordinates (e.g. [61]), we notice that the SEP terms affect (i) the ''Keplerian term'' on the first line, (ii) the tidal perturbations due to the other planets on the second line and (iii) produces an entirely new perturbation (the third line). This last term is of major importance. It is formally equivalent to an anomalous *indirect planetary perturbation*. For inner planets the contribution by Jupiter dominates the sum in the last line, so that this anomalous SEP perturbation is merely an acceleration in the heliocentric direction of Jupiter. The sensitivity to the η parameter depends basically on the solar compactness factor Ω_0 (with a very minor contribution $-\Omega_i$ of the ith planet). Since Ω_0 is so large, the planetary test of SEP is potentially very interesting. In the case of lunar laser ranging, the sensitivity on η is principally determined by the Earth value of Ω, four orders of magnitude smaller than Ω_0.

Note, however, that η is also present in the Keplerian term [the first line of Eq. (A3)]. Quantitatively, the contribution of η to the attraction from the Sun is not negligible [82]. However, this effect is identical to the effect of a change to the gravitational constant (or of the mass of the Sun, or of the value of the astronomical unit): $G\rightarrow G_\star = G\,[1+\eta\,\Omega_0]$. The planetary equations (A3) rewritten with $G_\star$ read

$$\frac{d^2\mathbf{q}_i}{dt^2} = -G_\star[1+\eta\Omega_i]\frac{M_0+M_i}{q_i^3}\mathbf{q}_i - \sum_{j\neq 0,i} G_\star[1+\eta\Omega_j]M_j\left(\frac{\mathbf{q}_{ij}}{q_{ij}^3}+\frac{\mathbf{q}_j}{q_j^3}\right) + \eta(\Omega_0-\Omega_i)\sum_{j\neq 0,i}\frac{G_\star M_j}{q_{ij}^3}\mathbf{q}_{ij}\,. \tag{A4}$$

The presence of the η terms in the first two lines in Eq. (A4) is negligible with the current observational accuracy. The principal perturbation allowing us to test the SEP is still the last term; moreover, since $|\Omega_0|\gg|\Omega_i|$ for any $i\geqslant 1$ we may adopt $\Omega_0-\Omega_i\approx\Omega_0$. Note that this SEP-testing term now appears as an anomalous *direct planetary perturbation*. Clearly, it is again dominated by the Jupiter influence, and over one year of the BepiColombo radio science experiment it is nearly a constant acceleration.

Adopting the approach of linear perturbations $\Delta\mathbf{q}_i$ of a reference solution (such as the planetary orbits from the JPL ephemerides), the SEP effect principally arrives from the forcing acceleration

$$\delta(d^2\mathbf{q}_i/dt^2)_\eta \simeq \eta\Omega_0\sum_{j\neq 0,i}\frac{G_\star M_j}{q_{ij}^3}\mathbf{q}_{ij}\,, \tag{A5}$$

with i standing for Mercury and Earth. Since in Eq. (10) we are using the barycentric coordinates, we then perform the transformation

$$\mathbf{r}_i = \mathbf{q}_i - \frac{1}{M}\sum_{j\neq 0} M_j\mathbf{q}_j\,, \tag{A6a}$$

$$\mathbf{r}_0 = -\frac{1}{M}\sum_{j\neq 0} M_j\mathbf{q}_j\,, \tag{A6b}$$

to obtain the corresponding perturbative accelerations in $\Delta\mathbf{r}_i$. These are then considered in the right-hand side of the system (10), together with other PN and solar perturbations.

We note that thanks to a combined reanalysis of the Voyager, Ulysses, Galileo and Cassini orbital tracking and a large number of the Earth-based astrometry the fractional uncertainty in the total mass of Jupiter's system has been recently decreased to $\simeq 8\times 10^{-9}$ [65]. This value is sufficiently small to prevent the uncertainty of the Newtonian gravitational perturbation due to Jupiter to affect the determination of η. Both effects are similar, but the indirect Jupiter's solar perturbation is enough to allow their decorrelation at this level of accuracy.

[1] D. Vokrouhlický, A. Milani, and S.R. Chesley, Icarus **148**, 118 (2000).

[2] D. Vokrouhlický and A. Milani, Astron. Astrophys. **362**, 746 (2000).

[3] R. Baum and W. Sheehan, *In Search of the Planet Vulcan—The Ghost in Newton's Clockwork Universe* (Plenum Press, New York, 1997).

[4] M.A. Leake, C.R. Chapman, S.J. Weidenschilling, D.R. Davis, and R. Greenberg, Icarus **71**, 350 (1987).

[5] S.A. Stern and D.D. Durda, Icarus **143**, 360 (2000).

[6] D. Vokrouhlický, P. Farinella, and W.F. Bottke, Icarus **148**, 147 (2000).

[7] A. Pais, *Subtle is the Lord. The Science and the Life of Albert Einstein* (Oxford University Press, Oxford, 1983).

[8] W. de Sitter, Mon. Not. R. Astron. Soc. **76**, 699 (1916); **77**, 155 (1916).

[9] C.M. Will, Living Rev. Relativ. **4**, 4 (2001).

[10] I.I. Shapiro, in *General Relativity and Gravitation*, edited by N. Ashby, D.F. Barlett, and W. Wyss (Cambridge University Press, Cambridge, England, 1990), p. 313.

[11] R.H. Dicke, Memoirs Amer. Philos. Soc. **78**, 1 (1970).

[12] C. Brans and R.H. Dicke, Phys. Rev. **124**, 925 (1961).

[13] C.M. Will, *Theory and Experiment in Gravitational Physics* (Cambridge University Press, Cambridge, England, 1981).

[14] T.J. Lydon and S. Sofia, Phys. Rev. Lett. **76**, 177 (1996).

[15] L. Paternó, S. Sofia, and M.P. DiMauro, Astron. Astrophys. **314**, 940 (1996).

[16] F.P. Pijpers, Mon. Not. R. Astron. Soc. **297**, L76 (1998).

[17] J.G. Williams, X.X. Newhall, and J.O. Dickey, Phys. Rev. D **53**, 6730 (1996).

[18] D.E. Lebach *et al.*, Phys. Rev. Lett. **75**, 1439 (1995).

[19] L. Iess, G. Giampieri, J.D. Anderson, and B. Bertotti, Class. Quantum Grav. **16**, 1487 (1999).

[20] T. Damour and G. Esposito-Farèse, Class. Quantum Grav. **9**, 2093 (1992).

[21] K. Nordtvedt, Phys. Rev. **169**, 1014 (1968); **169**, 1017 (1968).

[22] A.M. Nobili, in *Recent Advances in Metrology and Fundamental Constants*, edited by T.J. Quinn, S. Leschiutta, and P. Tavella (IOS Press, Amsterdam, 2001), p. 609.

[23] T. Damour and K. Nordtvedt, Phys. Rev. Lett. **70**, 2217 (1993).

[24] T. Damour and K. Nordtvedt, Phys. Rev. D **48**, 3436 (1993).

[25] P.L. Bender, N. Ashby, M.A. Vincent, and J.M. Wahr, Adv. Space Sci. **9**, 113 (1989).

[26] J.D. Anderson *et al.*, Planet. Space Sci. **45**, 21 (1997).

[27] N. Ashby, P.L. Bender, and J.M. Wahr, ''Gravitational physics tests from ranging to a small Mercury relativity satellite,'' preprint (1999).

[28] V. Iafolla and S. Nozzoli, Planet. Space Sci. **49**, 1609 (2001).

[29] L. Iess and G. Boscagli, Planet. Space Sci. **49**, 1597 (2001).

[30] A. Balogh *et al.*, BepiColombo: An interdisciplinary cornerstone mission to the planet Mercury, ESA-SCI(2000)1; see also http://sci.esa.int/home/bepicolombo/ for basic information about this mission, and http://solarsystem.estec.esa.nl/Mercury/MercuryAssess.htm for the System and Technology Study Report. Giuseppe (Bepi) Colombo (1920–1984) is credited, among many other achievements, for the theory explain-

ing Mercury's non-synchronous rotation, which was discovered with the first radar data from that planet.
[31] The mission will also include a "surface element," which is a semi-soft lander. Unfortunately, due to the harsh Mercury environment and to power problems, the lander is not planned to survive more than a week, thus a transponder would not be useful in determining either the orbit or the rotation of the planet.
[32] J.D. Anderson, M. Gross, K. Nordtvedt, and S.G. Turyshev, Astrophys. J. **459**, 365 (1996).
[33] A. Milani, A. Rossi, D. Vokrouhlický, D. Villani, and C. Bonanno, Planet. Space Sci. **49**, 1579 (2001).
[34] M.H. Soffel, *Relativity in Astrometry, Celestial Mechanics and Geodesy* (Springer, Berlin, 1989).
[35] S.A. Klioner and M.H. Soffel, Phys. Rev. D **62**, 024019 (2001).
[36] It might be worth mentioning that the JPL ephemerides in fact already contain partially the PPN analysis described below, since the lunar laser ranging and Viking data were used by JPL to constrain some of the PN parameters (e.g. $\overline{\gamma}$). However, since these results are so far in perfect agreement with general relativity and since the BepiColombo mission will be found to be able to constrain more tightly these parameters, we regard the JPL ephemerides as a pure general relativity template.
[37] K. Nordtvedt, Astrophys. J. **161**, 1059 (1970).
[38] K. Nordtvedt, Phys. Rev. D **3**, 1683 (1971).
[39] C.M. Will and K. Nordtvedt, Astrophys. J. **177**, 757 (1972).
[40] K. Nordtvedt and C.M. Will, Astrophys. J. **177**, 775 (1972).
[41] We disregard the PN parameter α_3 that besides the parametrizing dependence on the preferred cosmological frame also expresses a degree of violation of the conservation laws (e.g. [13]). Since these later effects are already of rather speculative character and since the parameter α_3 has been already very tightly constraint by the analysis of the binary pulsar dynamics [J.F. Bell, and T. Damour, Class. Quantum Grav. **13**, 3121 (1996)], in fact much more tightly than can be obtained from the Mercury data, the omission of this parameter from our analysis is justified.
[42] P.J.E. Peebles, *Principles of Physical Cosmology* (Princeton University Press, Princeton, 1993).
[43] D.J. Fixsen *et al.*, Astrophys. J. **420**, 445 (1994).
[44] C.H. Lineweaver *et al.*, Astrophys. J. **470**, 38 (1996).
[45] T. Damour and G. Esposito-Farèse, Phys. Rev. D **49**, 1693 (1994).
[46] T. Damour and G. Esposito-Farèse, Phys. Rev. D **50**, 2381 (1994).
[47] M.E. Davies *et al.*, Celest. Mech. Dyn. Astron. **53**, 377 (1992).
[48] D.K. Yeomans *et al.*, Astron. J. **103**, 303 (1992).
[49] R.W. Hellings, Astron. J. **91**, 650 (1986).
[50] G.W. Richter and R.A. Matzner, Phys. Rev. D **28**, 3007 (1983).
[51] B. Bertotti and G. Giampieri, Class. Quantum Grav. **9**, 777 (1992).
[52] B. Bertotti, G. Comoretto, and L. Iess, Astron. Astrophys. **269**, 608 (1993).
[53] L. Iess (personal communication).
[54] The measurements are taken from some ground stations, but the geocentric position and rotation of the stations are well known, e.g., by VLBI and other techniques, thus in the discussion which follows we will assume that an accurate topocentric correction has been applied and the observations are considered to be from the center of mass of the Earth.
[55] A. Milani, M. Carpino, A. Rossi, G. Catastini, and S. Usai, Manuscripta Geodaetica **20**, 123 (1995).
[56] Time-dependent phenomena, such as tides, have to be parametrized with time-independent coefficients, such as Love numbers.
[57] Even if there were significant correlations between local and global parameters, a two step procedure could be used, but in this case the sequence of two steps should be considered as one iteration in an iterative process, to be repeated until convergence.
[58] A symmetric positive definite matrix is badly conditioned if the ratio between the largest and the smallest eigenvalue is large.
[59] C. Bonanno and A. Milani, Celest. Mech. Dyn. Astron. **83**, 17 (2002).
[60] The group of symmetries is assumed to act effectively; that is, no subgroup larger than the identity acts trivially.
[61] A.E. Roy, *Orbital Motion* (Hilger Ltd, Bristol, 1982).
[62] A. Milani and A.M. Nobili, Celest. Mech. **31**, 241 (1983).
[63] The results are somewhat sensitive to the choice of the reference time t_0. The figures and tables in this paper refer to tests done with t_0 set to the initial time (at the beginning of the orbital phase of the BepiColombo mission). Because of the particular shape of the systematic range drift, the more usual choice of t_0 at the center of the observation time span does not give better results for all parameters, actually somewhat worse in the case with preferred frame parameters.
[64] A change in distance ΔR_i can be the effect of the corrections to the positions of both planets; the fact that, in the multiarc fit, it was obtained by displacing only Mercury in the Earth-Mercury direction does not matter, because a motion of the Earth would produce exactly the same effects.
[65] R.A. Jacobson, Bull. Am. Astron. Soc. **33**, 1101 (2001); a small improvement can be expected if the data from the Europa Orbiter mission, scheduled presently for 2008, were available [R.A. Jacobson (private communication)].
[66] Compare with the discussion of the "matrix-inversion limitations" in M.E. Ash, I.I. Shapiro, and W.B. Smith, Astron. J. **72**, 338 (1967).
[67] L.D. Landau and E.M. Lifschitz, *Méchanique* (Éditions MIR, Moscow, 1966).
[68] T.M. Eubanks *et al.*, Advances in solar system tests of gravity, preprint available at http://casa.usno.navy.mil/navnet/postscript, file prd_15.ps.
[69] J. Chapront and F. Mignard, C. R. Acad. Sci. Paris, Série IV **10**, 1233 (2000).
[70] R.W. Hellings *et al.*, Phys. Rev. Lett. **51**, 1609 (1983).
[71] R.W. Hellings, in *General Relativity and Gravitation*, edited by B. Bertotti, F. de Felice, and A. Pascolini (Reidel, Dordrecht, 1984), p. 365.
[72] J. Muller, K. Nordtvedt, and D. Vokrouhlický, Phys. Rev. D **54**, 5927 (1996).
[73] J.F. Bell, F. Camilo, and T. Damour, Astrophys. J. **464**, 857 (1996).
[74] K. Nordtvedt, Astrophys. J. **320**, 871 (1987).
[75] The solar equator does not coincide with either the ecliptic or with the invariant plane of the solar system. The inclination of

the orbit of Mercury with respect to the solar equator is less than half of the inclination of the same orbit with respect to the ecliptic: see [47].
[76] K. Nordtvedt, Phys. Rev. D **61**, 122001 (2000).
[77] In Ref. [27] there is a discussion of the possible effects of the ''asteroid noise'' on the determination of some PN parameters, but their ''worst case analysis'' is too pessimistic, providing only a loose upper bound for this effect.
[78] The first tests with a complete 5-way link have shown that it is possible to achieve range rate measurements with accuracies of the order of 6 μm/s (for integration time 1000 s) down to 8 solar radii; L. Iess (private communication).
[79] K. Nordtvedt, Astrophys. J. **297**, 390 (1985).
[80] K. Nordtvedt, Astrophys. J. **407**, 758 (1993).
[81] If the range drift flattens out after about one year, then the second year of data would be very useful. But, if this is the case, then the transponder should be turned on during the cruise phase, so that the drift takes place before the beginning of the orbital phase (if the calibration was a constant it could be easily eliminated in the data processing, as we have done for the SCE).
[82] The astronomical unit is known today to an accuracy of ± 6 m, which fractionally means $\approx 4\times 10^{-11}$. This accuracy is comparable to the η correction from the first line of Eq. (A3) (given the limit $|\eta|<10^{-3}$ from lunar laser ranging, Ref. [17]).